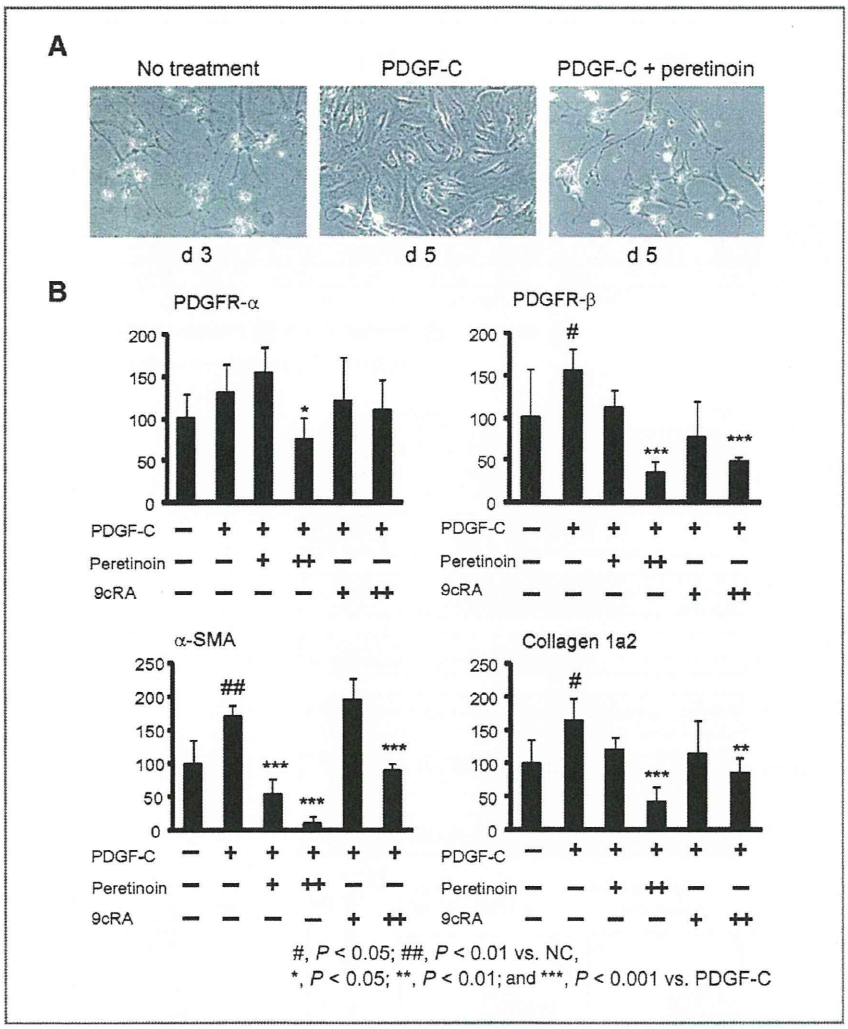

Figure 5. A, microscopic view of freshly isolated primary mouse HSCs after PDGF-C transformation into myofibroblasts (left). Peretinoin inhibited the transformation of HSCs by PDGF-C. B, RTD-PCR analysis of PDGFR-α, PDGFR-β, α-SMA, and collagen 1a2 expression in HSCs treated with or without PDGF-C, peretinoin, and 9cRA ($n = 4$). PDGF-C (+), 80 ng/mL; peretinoin (+), 5 μmol/L; (++), 10 μmol/L; 9cRA (+), 5 μmol/L; (++), 10 μmol/L. NC, no control.

signaling is activated in hepatic tumors and repressed by peretinoin.

Growth factors such as PDGF or HGF potentially activate Wnt/β-catenin signaling (26, 28), which promotes cancer progression and metastasis. We evaluated whether such growth factor signaling could be repressed by peretinoin in hepatic tumors. The expression of c-myc, β-catenin, Tie2, Fit-1, and Flk-1 were significantly upregulated from 1.5- to 4-fold in hepatic tumors compared with normal liver, and this expression was significantly repressed by peretinoin. Similarly, the expression of PDGFR-α, PDGFR-β, collagen 1a2, collagen 4a2, tissue inhibitor of metalloproteinase 2 (TIMP2), and cyclin D1 was substantially upregulated from 5- to 15-fold in hepatic tumors, and significantly repressed by peretinoin (Fig. 7D). Thus, growth factor signaling as well as canonical Wnt/β-catenin signaling in hepatic tumors seems to be repressed by peretinoin. These results explain the inhibitory effect of peretinoin in the development of HCC in *Pdgf-c Tg* mice.

Discussion

HCC often develops in association with liver cirrhosis and its high recurrence rate leads to poor patient prognosis. Indeed, the 10-year recurrence-free survival rate after liver resection for HCC with curative intent was shown to be only 20% (29). Therefore, there is a pressing need to develop effective preventive therapy for HCC recurrence to improve its prognosis.

Peretinoin, a member of the acyclic retinoid family, is expected to be an effective chemopreventive drug for HCC (11, 12, 30) as shown by a previous phase II/III trial in which 600 mg peretinoin per day in the Child-Pugh A subgroup reduced the risk of HCC recurrence or death by 40% [HR = 0.60 (95% CI, 0.40–0.89); ref. 31]. However, further clinical

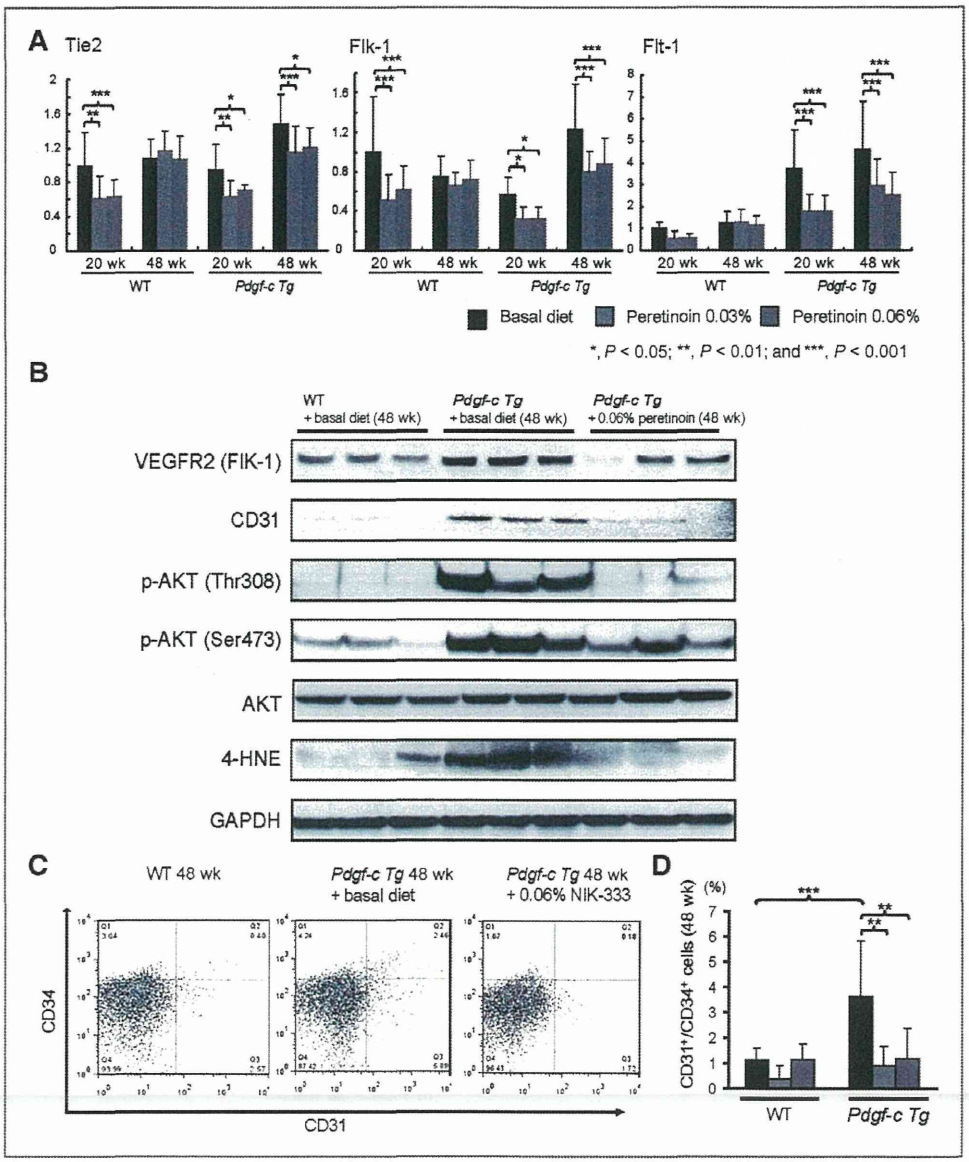

Figure 6. A, RTD-PCR analysis of Tie2, Flk-1, and Flt-1 expression in the liver of *Pdgf-c Tg* and WT mice fed with different diets ($n = 15$). B, Western blotting of Flk-1, CD31, p-AKT (Thr 308, Ser473), AKT, 4-HNE, and GAPDH expression in the liver of *Pdgf-c Tg* or WT mice fed a basal diet or 0.06% peretinoin at 48 weeks ($n = 3$). C, fluorescence-activated cell-sorting analysis of CD31- and CD34-positive CEC in blood of *Pdgf-c Tg* or WT mice fed a basal diet or 0.06% peretinoin at 48 weeks. D, frequency of CD31- and CD34-positive CEC in blood of *Pdgf-c Tg* or WT mice fed a basal diet or 0.06% peretinoin at 48 weeks ($n = 10$).

studies are needed to confirm the clinical efficacy of peretinoin, and a large scale study involving several countries is currently being planned.

During the course of chronic hepatitis, nonparenchymal cells including Kupffer, endothelial and activated stellate cells release a variety of cytokines and growth factors that might accelerate hepatocarcinogenesis. Although peretinoin has been shown to suppress the growth of HCC-derived cells by inducing apoptosis and differentiation (32–35), increasing p21 and reducing cyclin D1 (13), limited data have been published about its effects on hepatic mesenchymal cells such as stellate cells and endothelial cells (14).

In parallel with a phase II/III trial, we conducted a pharmacokinetics study of peretinoin focusing on 12

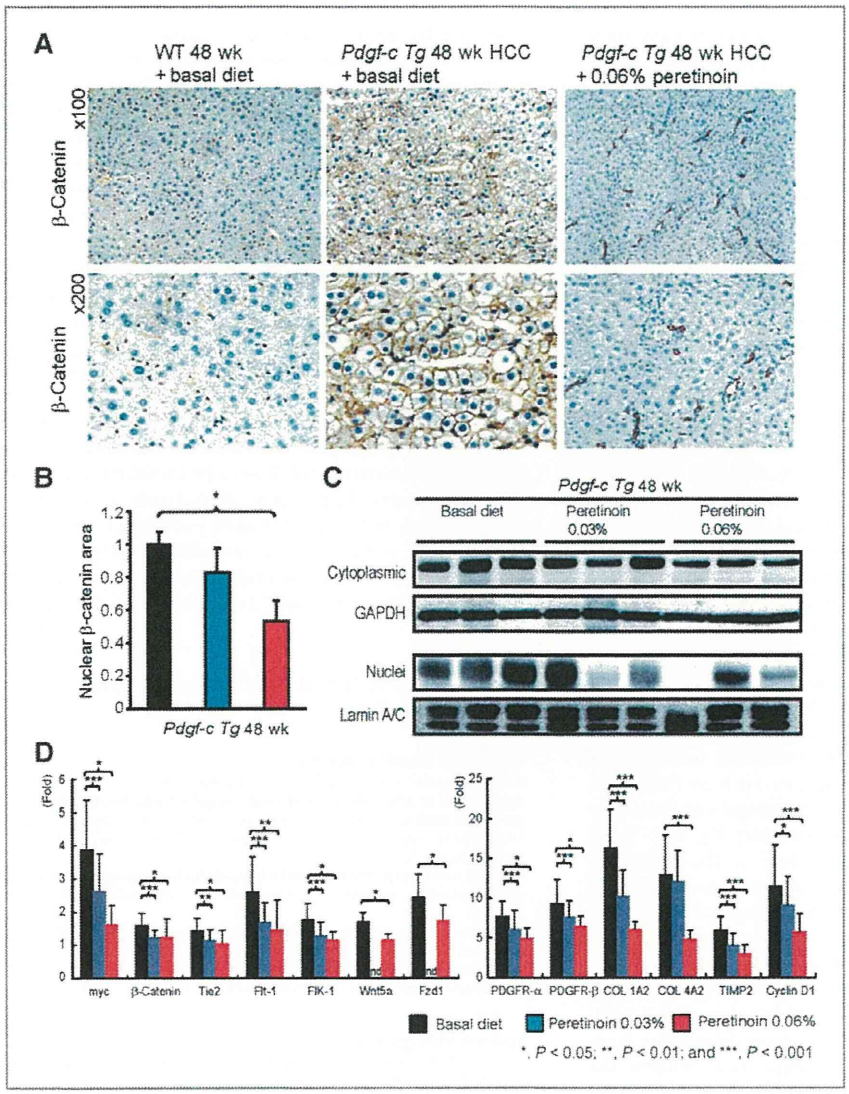

Figure 7. A, IHC staining of β-catenin expression in HCC tissues of *Pdgf-c Tg* mice fed a basal diet or 0.06% peretinoin at 48 weeks. B, densitometric analysis of β-catenin expression in the liver of *Pdgf-c Tg* mice fed with different diets ($n = 15$ for basal diet, $n = 15$ for 0.03% peretinoin, $n = 5$ for 0.06% peretinoin). C, Western blotting of β-catenin expression in cytoplasmic and nuclear fractions of *Pdgf-c Tg* mouse livers fed with different diets. GAPDH was used to standardize cytoplasmic protein and lamin A/C to standardize nuclear protein ($n = 3$). D, RTD-PCR analysis of myc, β-catenin, Tie2, Flt-1, Flk-1, Wnt5a, Fzd1, PDGFR-α, PDGFR-β, collagen (COL) 1a2, collagen 4a2, TIMP2, and cyclin D1 expression in HCC tissues of *Pdgf-c Tg* mice fed with different diets ($n = 15$ for basal diet, $n = 15$ for 0.03% peretinoin, $n = 5$ for 0.06% peretinoin). Relative fold expressions compared with WT mice are shown.

patients with CH-C and HCC to monitor the biological behavior of peretinoin in the liver. Gene expression profiling during peretinoin administration revealed that HCC recurrence within 2 years could be predicted and that PDGF-C expression was one of the strongest predictors. In addition, other genes related to angiogenesis, cancer stem cell and tumor progression were downregulated, whereas expression of genes related to hepatocyte differentiation and tumor suppression was upregulated by peretinoin (data not shown). Moreover, a recent report revealed the emerging significance of PDGF-C–mediated angiogenic and tumorigenic properties (7, 8, 36). In this study, we therefore used the mouse model of *Pdgf-c Tg*, which displays the phenotypes of hepatic fibrosis, steatosis, and HCC development that resemble human HCC arising from chronic hepatitis usually associated with advanced hepatic fibrosis.

We showed that peretinoin effectively inhibits the progression of hepatic fibrosis and tumors in *Pdgf-c Tg* mice (Figs. 1 and 4). Affymetrix gene chips analysis revealed dynamic changes in hepatic gene expression (Supplementary Fig. S3), which were confirmed by IHC staining, RTD-PCR and Western blotting. Pathway analysis of differentially expressed genes suggested that the transcriptional regulators Sp1 and Ap1 are key regulators in the peretinoin inhibition of hepatic fibrosis and tumor development in *Pdgf-c Tg* mice (Supplementary Fig. S5).

We clearly showed that peretinoin inhibited PDGF signaling through the inhibition of PDGFRs (Figs. 2 and 3). In

addition, we showed that PDGFR repression by peretinoin inhibited primary stellate cell activation (Fig. 5). Interestingly, this inhibitory effect was more pronounced than the effects of 9cRA (Fig. 5B). Normal mouse and human hepatocytes neither express PDGF receptors (J.S. Campbell and N. Fausto, unpublished data), nor proliferate in response to treatment with PDGF ligands (7). However, peretinoin inhibited the expression of PDGFRs, collagens, and their downstream signaling molecules in cell lines of hepatoma (Huh-7, HepG2, and HLE), fibroblast (NIH3T3), endothelial cells (HUVEC), and stellate cells (Lx-2; Supplementary Fig. S6). Furthermore, Sp1 but not Ap1, might be involved in the repression of PDGFR-α in Huh-7 cells (Supplementary Fig. 6C). The overexpression of Sp1-activated PDGFR-α promoter activity, whereas siRNA knockdown of Sp1 repressed PDGFR-α promoter activity in Huh-7 cells (data not shown). Therefore, this seems to confirm that Sp1 is involved in the regulation of PDGFR, as reported previously (37, 38), although these findings should be further investigated in different cell lines. A recent report showed the involvement of transglutaminase 2, caspase3, and Sp1 in peretinoin signaling (35).

Peretinoin was shown to inhibit angiogenesis in the liver of *Pdgf-c Tg* mice in this study, as shown by the decreased expression of VEGFR1/2 and Tie 2 (Figs. 2 and 6 and Supplementary Fig. S1). Moreover, peretinoin inhibited the number of $CD31^+$ and $CD34^+$ endothelial cells (CEC) in the blood and liver (Fig. 6C and D), while also inhibiting the expression of EGFR, c-kit, PDGFRs, and VEGFR1/2 in *Pdgf-c Tg* mice (data not shown). We also showed that peretinoin inhibited the expression of multiple growth factors such as HGF, IGF, VEGF, PDGF, and HDGF, which were upregulated from 3- to 10-fold in *Pdgf-c Tg* mice (Supplementary Fig. S3). These activities collectively might contribute to the antitumor effect of peretinoin in *Pdgf-c Tg* mice. The inhibition of both PDGFRs and VEGFR signaling by peretinoin was previously shown to have a significant effect on tumor growth (36), and we confirmed herein that peretinoin inhibited the expression of VEGFR2 in HUVECs (Supplementary Fig. S6; ref. 39). Finally, we showed that peretinoin inhibited canonical Wnt/β-catenin signaling by showing the decreased nuclear accumulation of β-catenin (Fig. 7). These data confirm the previous hypothesis of transrepression of the β-catenin promoter by 9cRA *in vitro* (40).

Although we showed that the PDGF signaling pathway is a target of peretinoin for preventing the development of hepatic fibrosis and tumors in mice, retinoid-inducing genes such as G0S2 (41), TGM2 (35), CEBPA (42), ATF, TP53BP, metallothionein 1H (MT1H), MT2A, and hemopexin (HPX) were upregulated in peretinoin-treated mice (data not shown). These canonical retinoid pathways are likely to participate in preventing disease progression in conjunction with anti-PDGF effects.

The precise mechanism of peretinoin toxicity, in which 5% of mice treated with 0.06% peretinoin died after 24 weeks of treatment, is currently under investigation. These mice showed severe osteopenia and we speculate that the toxicity might be caused by retinoid-induced osteopenia, as observed in a hypervitaminosis A rat model (43). However, the toxicity of prolonged treatment with oral retinoids in humans remains controversial (44) and severe osteopenia has so far only been seen in a rodent model.

In summary, we show that peretinoin effectively inhibits hepatic fibrosis and HCC development in *Pdgf-c Tg* mice. Further studies are needed to elucidate the detailed molecular mechanisms of peretinoin action and the effect of peretinoin on PDGF-C in human HCC. The recently developed multikinase inhibitor Sorafenib (BAY 43-9006, Nexavar) was shown to improve the prognosis of patients with advanced HCC (45). Promisingly, a phase II/III trial of peretinoin showed it to be safe and well tolerated (46). Therefore, combinatorial therapy that incorporates the use of small molecule inhibitors with peretinoin may be beneficial to some patients. The application of peretinoin during pre- or early-fibrosis stage could be beneficial in preventing the progression of fibrosis and subsequent development of HCC in patients with chronic liver disease.

Disclosure of Potential Conflicts of Interest

No potential conflicts of interest were disclosed.

Authors' Contributions

Conception and design: M. Honda, J.S. Campbell, S. Kaneko
Acquisition of data (provided animals, acquired and managed patients, provided facilities, etc.): H. Okada, M. Honda, J.S. Campbell, Y. Sakai, T. Yamashita, Y. Takebuchi, K. Hada, T. Shirasaki, R. Takabatake, M. Nakamura, H. Sunagozaka, N. Fausto
Analysis and interpretation of data (e.g., statistical analysis, biostatistics, computational analysis): J.S. Campbell, T. Yamashita, H. Sunagozaka, S Kaneko
Writing, review, and/or revision of the manuscript: H. OkadaM. Honda, J.S. Campbell, N. Fausto, S. Kaneko
Study supervision: J.S. Campbell, S. Kaneko
Pathologic examination and evaluation: T. Tanaka

Acknowledgments

The authors thank Dr. Scott Friedman, Mount Sinai School of Medicine (New York, NY), for providing Lx-2 cell lines and Nami Nishiyama and Masayo Baba for their excellent technical assistance.

Grant Support

This work was funded by NIH grants CA-23226, CA-174131, and CA-127228 (J.S. Campbell and N. Fausto). This work was also supported in part by a grant-in-aid from the Ministry of Health, Labour and Welfare, and KOWA Co., Ltd., Tokyo, Japan (M. Honda and colleagues).

The costs of publication of this article were defrayed in part by the payment of page charges. This article must therefore be hereby marked *advertisement* in accordance with 18 U.S.C. Section 1734 solely to indicate this fact.

Received January 9, 2012; revised April 27, 2012; accepted May 18, 2012; published OnlineFirst May 31, 2012.

References

1. Befeler AS, Di Bisceglie AM. Hepatocellular carcinoma: diagnosis and treatment. Gastroenterology 2002;122:1609–19.
2. Mohamed AE, Kew MC, Groeneveld HT. Alcohol consumption as a risk factor for hepatocellular carcinoma in urban southern African blacks. Int J Cancer 1992;51:537–41.

3. Tsukuma H, Hiyama T, Tanaka S, Nakao M, Yabuuchi T, Kitamura T. et al. Risk factors for hepatocellular carcinoma among patients with chronic liver disease. N Engl J Med 1993; 328:1797–801.
4. Deugnier YM, Charalambous P, Le Quilleuc D, Turlin B, Searle J, Brissot P, et al. Preneoplastic significance of hepatic iron-free foci in genetic hemochromatosis: a study of 185 patients. Hepatology 1993;18:1363–9.
5. Yeoman AD, Al-Chalabi T, Karani JB, Quaglia A, Devlin J, Mieli-Vergani G, et al. Evaluation of risk factors in the development of hepatocellular carcinoma in autoimmune hepatitis: implications for follow-up and screening. Hepatology 2008;48:863–70.
6. Smedile A, Bugianesi E. Steatosis and hepatocellular carcinoma risk. Eur Rev Med Pharmacol Sci 2005;9:291–3.
7. Campbell JS, Hughes SD, Gilbertson DG, Palmer TE, Holdren MS, Haran AC, et al. Platelet-derived growth factor C induces liver fibrosis, steatosis, and hepatocellular carcinoma. Proc Natl Acad Sci U S A 2005;102:3389–94.
8. Crawford Y, Kasman I, Yu L, Zhong C, Wu X, Modrusan Z, et al. PDGF-C mediates the angiogenic and tumorigenic properties of fibroblasts associated with tumors refractory to anti-VEGF treatment. Cancer Cell 2009;15:21–34.
9. Lau DT, Luxon BA, Xiao SY, Beard MR, Lemon SM. Intrahepatic gene expression profiles and alpha-smooth muscle actin patterns in hepatitis C virus induced fibrosis. Hepatology 2005;42: 273–81.
10. Honda M, Yamashita T, Ueda T, Takatori H, Nishino R, Kaneko S. Different signaling pathways in the livers of patients with chronic hepatitis B or chronic hepatitis C. Hepatology 2006;44: 1122–38.
11. Muto Y, Moriwaki H, Ninomiya M, Adachi S, Saito A, Takasaki KT, et al. Prevention of second primary tumors by an acyclic retinoid, polyprenoic acid, in patients with hepatocellular carcinoma. Hepatoma Prevention Study Group. N Engl J Med 1996;334:1561–7.
12. Muto Y, Moriwaki H, Saito A. Prevention of second primary tumors by an acyclic retinoid in patients with hepatocellular carcinoma. N Engl J Med 1999;340:1046–7.
13. Suzui M, Masuda M, Lim JT, Albanese C, Pestell RG, Weinstein IB. Growth inhibition of human hepatoma cells by acyclic retinoid is associated with induction of p21(CIP1) and inhibition of expression of cyclin D1. Cancer Res 2002;62:3997–4006.
14. Sano T, Kagawa M, Okuno M, Ishibashi N, Hashimoto M, Yamamoto M, et al. Prevention of rat hepatocarcinogenesis by acyclic retinoid is accompanied by reduction in emergence of both TGF-alpha-expressing oval-like cells and activated hepatic stellate cells. Nutr Cancer 2005;51:197–206.
15. Muto Y, Moriwaki H, Omori M. *In vitro* binding affinity of novel synthetic polyprenoids (polyprenoic acids) to cellular retinoid-binding proteins. Gann 1981;72:974–7.
16. Yamada Y, Shidoji Y, Fukutomi Y, Ishikawa T, Kaneko T, Nakagama H, et al. Positive and negative regulations of albumin gene expression by retinoids in human hepatoma cell lines. Mol Carcinog 1994;10:151–8.
17. Honda M, Sakai A, Yamashita T, Nakamoto Y, Mizukoshi E, Sakai Y, et al. Hepatic ISG expression is associated with genetic variation in interleukin 28B and the outcome of IFN therapy for chronic hepatitis C. Gastroenterology 2010;139:499–509.
18. Frith C, Ward J, Turusov V. Pathology of tumors in laboratory animals. Vol. 2. Lyon, France: IARC Scientific Publications; 1994. p. 223–70.
19. Thoolen B, Maronpot RR, Harada T, Nyska A, Rousseaux C, Nolte T, et al. Proliferative and nonproliferative lesions of the rat and mouse hepatobiliary system. Toxicol Pathol 2010;38: 5S–81S.
20. Honda M, Takehana K, Sakai A, Tagata Y, Shirasaki T, Nishitani S, et al. Malnutrition impairs interferon signaling through mTOR and FoxO pathways in patients with chronic hepatitis C. Gastroenterology 2011;141:128–40, 140.e1–2.
21. Frith CH, Ward JM, Turusov VS. Tumours of the liver. IARC Sci Publ 1994;111:223–69.
22. Xu L, Hui AY, Albanis E, Arthur MJ, O'Byrne SM, Blaner WS, et al. Human hepatic stellate cell lines, LX-1 and LX-2: new tools for analysis of hepatic fibrosis. Gut 2005;54:142–51.
23. Nhieu JT, Renard CA, Wei Y, Cherqui D, Zafrani ES, Buendia MA. Nuclear accumulation of mutated beta-catenin in hepatocellular carcinoma is associated with increased cell proliferation. Am J Pathol 1999;155:703–10.
24. Wong CM, Fan ST, Ng IO. beta-Catenin mutation and overexpression in hepatocellular carcinoma: clinicopathologic and prognostic significance. Cancer 2001;92:136–45.
25. van Zijl F, Mair M, Csiszar A, Schneller D, Zulehner G, Huber H, et al. Hepatic tumor-stroma crosstalk guides epithelial to mesenchymal transition at the tumor edge. Oncogene 2009;28: 4022–33.
26. Fischer AN, Fuchs E, Mikula M, Huber H, Beug H, Mikulits W. PDGF essentially links TGF-beta signaling to nuclear beta-catenin accumulation in hepatocellular carcinoma progression. Oncogene 2007;26: 3395–405.
27. Hou X, Kumar A, Lee C, Wang B, Arjunan P, Dong L, et al. PDGF-CC blockade inhibits pathological angiogenesis by acting on multiple cellular and molecular targets. Proc Natl Acad Sci U S A 2010;107: 12216–21.
28. Apte U, Zeng G, Muller P, Tan X, Micsenyi A, Cieply B, et al. Activation of Wnt/beta-catenin pathway during hepatocyte growth factor-induced hepatomegaly in mice. Hepatology 2006;44:992–1002.
29. Eguchi S, Kanematsu T, Arii S, Omata M, Kudo M, Sakamoto M, et al. Recurrence-free survival more than 10 years after liver resection for hepatocellular carcinoma. Br J Surg 2011;98:552–7.
30. Okusaka T, Ueno H, Ikeda M, Morizane C. Phase I and pharmacokinetic clinical trial of oral administration of the acyclic retinoid NIK-333. Hepatol Res 2011;41:542–52.
31. Okusaka T, Makuuchi M, Matsui O, Kumada H, Tanaka K, Kaneko S, et al. Clinical benefit of peretinoin for the suppression of hepatocellular carcinoma (HCC) recurrence in patients with Child-Pugh grade A (CP-A) and small tumor: a subgroup analysis in a phase II/III randomized, placebo-controlled trial. J Clin Oncol 2011;29 Suppl 4s:165.
32. Araki H, Shidoji Y, Yamada Y, Moriwaki H, Muto Y. Retinoid agonist activities of synthetic geranyl geranoic acid derivatives. Biochem Biophys Res Commun 1995;209:66–72.
33. Nakamura N, Shidoji Y, Yamada Y, Hatakeyama H, Moriwaki H, Muto Y. Induction of apoptosis by acyclic retinoid in the human hepatoma-derived cell line, HuH-7. Biochem Biophys Res Commun 1995;207: 382–8.
34. Yasuda I, Shiratori Y, Adachi S, Obora A, Takemura M, Okuno M, et al. Acyclic retinoid induces partial differentiation, down-regulates telomerase reverse transcriptase mRNA expression and telomerase activity, and induces apoptosis in human hepatoma-derived cell lines. J Hepatol 2002;36:660–71.
35. Tatsukawa H, Sano T, Fukaya Y, Ishibashi N, Watanabe M, Okuno M, et al. Dual induction of caspase 3- and transglutaminase-dependent apoptosis by acyclic retinoid in hepatocellular carcinoma cells. Mol Cancer 2011;10:4.
36. Timke C, Zieher H, Roth A, Hauser K, Lipson KE, Weber KJ, et al. Combination of vascular endothelial growth factor receptor/platelet-derived growth factor receptor inhibition markedly improves radiation tumor therapy. Clin Cancer Res 2008;14: 2210–9.
37. Molander C, Hackzell A, Ohta M, Izumi H, Funa K. Sp1 is a key regulator of the PDGF beta-receptor transcription. Mol Biol Rep 2001;28: 223–33.
38. Bonello MR, Khachigian LM. Fibroblast growth factor-2 represses platelet-derived growth factor receptor-alpha (PDGFR-alpha) transcription via ERK1/2-dependent Sp1 phosphorylation and an atypical cis-acting element in the proximal PDGFR-alpha promoter. J Biol Chem 2004;279:2377–82.
39. Komi Y, Sogabe Y, Ishibashi N, Sato Y, Moriwaki H, Shimokado K, et al. Acyclic retinoid inhibits angiogenesis by suppressing the MAPK pathway. Lab Invest 2010;90:52–60.

40. Shah S, Hecht A, Pestell R, Byers SW. Trans-repression of beta-catenin activity by nuclear receptors. J Biol Chem 2003;278: 48137–45.
41. Kitareewan S, Blumen S, Sekula D, Bissonnette RP, Lamph WW, Cui Q, et al. G0S2 is an all-trans-retinoic acid target gene. Int J Oncol 2008;33:397–404.
42. Uray IP, Shen Q, Seo HS, Kim H, Lamph WW, Bissonnette RP, et al. Rexinoid-induced expression of IGFBP-6 requires RARbeta-dependent permissive cooperation of retinoid receptors and AP-1. J Biol Chem 2009;284:345–53.
43. Hough S, Avioli LV, Muir H, Gelderblom D, Jenkins G, Kurasi H, et al. Effects of hypervitaminosis A on the bone and mineral metabolism of the rat. Endocrinology 1988;122: 2933–9.
44. Ribaya-Mercado JD, Blumberg JB. Vitamin A: is it a risk factor for osteoporosis and bone fracture? Nutr Rev 2007;65: 425–38.
45. Llovet JM, Ricci S, Mazzaferro V, Hilgard P, Gane E, Blanc JF, et al. Sorafenib in advanced hepatocellular carcinoma. N Engl J Med 2008;359:378–90.
46. Okita K, Matsui O, Kumada H, Tanaka K, Kaneko S, Moriwaki H, et al. Effect of peretinoin on recurrence of hepatocellular carcinoma (HCC): results of a phase II/III randomized placebo-controlled trial. J Clin Oncol 2010;28 Suppl 15s:4024.

Malnutrition Impairs Interferon Signaling Through mTOR and FoxO Pathways in Patients With Chronic Hepatitis C

MASAO HONDA,[*,‡] KENJI TAKEHANA,[§] AKITO SAKAI,[*] YUSUKE TAGATA,[§] TAKAYOSHI SHIRASAKI,[‡] SHINOBU NISHITANI,[§] TAKAHIKO MURAMATSU,[‖] TATSUYA YAMASHITA,[*] YASUNARI NAKAMOTO,[*] EISHIRO MIZUKOSHI,[*] YOSHIO SAKAI,[*] TARO YAMASHITA,[*] MIKIKO NAKAMURA,[*] TETSURO SHIMAKAMI,[¶] MINKYUNG YI,[#] STANLEY M. LEMON,[¶] TETSUO SUZUKI,[**] TAKAJI WAKITA,[**] SHUICHI KANEKO,[*] and the Hokuriku Liver Study Group

*Department of Gastroenterology, ‡Department of Advanced Medical Technology, Kanazawa University Graduate School of Medicine, Kanazawa, Japan; §Exploratory Research Laboratories, Research Center, Ajinomoto Pharmaceuticals, Co, Ltd, Kanagawa, Japan; Frontier Research Labs, Institute for Innovation, Ajinomoto, Co, Inc, Kanagawa, Japan; ¶Division of Infectious Diseases, School of Medicine, The University of North Carolina at Chapel Hill, Chapel Hill, North Carolina; #Center for Hepatitis Research, Institute for Human Infections and Immunity, and Department of Microbiology and Immunology, University of Texas Medical Branch, Galveston, Texas; and **Department of Virology II, National Institute of Infectious Diseases, Tokyo, Japan

CLINICAL LIVER

BACKGROUND & AIMS: Patients with advanced chronic hepatitis C (CH-C) often are malnourished, but the effects of malnutrition on interferon (IFN) signaling and response to treatment have not been determined. We assessed the importance of the nutritional state of the liver on IFN signaling and treatment response. **METHODS:** We studied data from 168 patients with CH-C who were treated with the combination of pegylated-IFN and ribavirin. Plasma concentrations of amino acids were measured by mass spectrometry. Liver gene expression profiles were obtained from 91 patients. Huh-7 cells were used to evaluate the IFN signaling pathway, mammalian target of rapamycin complex 1 (mTORC1), and forkhead box O (FoxO). Antiviral signaling induced by branched-chain amino acids (BCAAs) was determined using the in vitro hepatitis C virus replication system. **RESULTS:** Multivariate logistic regression analysis showed that Fischer's ratio was associated significantly with nonresponders, independent of interleukin-28B polymorphisms or the histologic stage of the liver. Fischer's ratio was correlated inversely with the expression of BCAA transaminase 1, and was affected by hepatic mTORC1 signaling. IFN stimulation was impaired substantially in Huh-7 cells grown in medium that was low in amino acid concentration, through repressed mTORC1 signaling, and increased Socs3 expression, which was regulated by Foxo3a. BCAA could restore impaired IFN signaling and inhibit hepatitis C virus replication under conditions of malnutrition. **CONCLUSIONS: Malnutrition impaired IFN signaling by inhibiting mTORC1 and activating Socs3 signaling through Foxo3a. Increasing BCAAs to up-regulate IFN signaling might be used as a new therapeutic approach for patients with advanced CH-C.**

Keywords: HCV; Liver Disease; Therapy; Diet.

Interferon (IFN) and ribavirin (RBV) combination therapy is a popular modality for treating patients with chronic hepatitis C (CH-C), but approximately 50% of patients usually relapse, particularly those with hepatitis C virus (HCV) genotype 1b and a high viral load.[1]

Recent landmark studies of genome-wide associations identified genomic loci associated with treatment responses to pegylated (Peg)-IFN and RBV combination therapy,[2,3] and a polymorphism in the interleukin (IL)-28B gene was found to predict hepatitis C treatment-induced viral clearance. Moreover, we previously showed that expression of hepatic IFN-stimulated genes (ISGs) was associated with the IL-28B polymorphism and might contribute to the treatment response.[4] In addition to the IL-28B polymorphism, host factors such as fibrosis stage and metabolic status of the liver might be associated with the treatment outcome[4,5]; however, the significance of these factors in conjunction with the IL-28B polymorphism has not been evaluated fully.

In CH-C livers, prolonged liver cell damage, fibrosis development, and microcirculation failure can lead to a state of malnutrition in hepatocytes, resulting in the impairment of multiple metabolic pathways. In patients with advanced stage CH-C, hypoalbuminemia and decreased plasma values for the Fischer's ratio of branched-amino acids (BCAA; leucine, isoleucine, and valine) to aromatic amino acids (tyrosine and phenylalanine) commonly are observed. BCAA are the essential amino acids necessary for ammonium metabolism in muscle when the liver is unable to perform this function. Recent reports have shown that BCAA activates albumin synthesis in rat

Abbreviations used in this paper: BCAA, branched-chain amino acid; BCAT1, branched chain amino-acid transaminase 1; CH-C, chronic hepatitis C; ChIP, chromatin immunoprecipitation; DMEM, Dulbecco's modified Eagle medium; FBE, Foxo binding element; FBEmut, Foxo binding element mutant; FoxO, forkhead box, subgroup O; GLuc, Gaussia luciferase; IFN, interferon; IL, interleukin; ISG, interferon-stimulated genes; mTOR, mammalian target of rapamycin; mTORC1, mammalian target of rapamycin complex 1; NR, no response; PCR, polymerase chain reaction; Peg, pegylated; p-mTOR, phosphorylated form of mammalian target of rapamycin; pS6K, phosphorylated form of p70 S6 protein kinase; pSTAT1, phosphorylated form of signal transducer and activator of transcription 1; Raptor, regulatory associated protein of mTOR; RBV, ribavirin; S6K, p70 S6 protein kinase; siRNA, small interfering RNA; SVR, sustained viral response; TR, transient response.

0016-5085/$36.00
doi:10.1053/j.gastro.2011.03.051

primary hepatocytes[6] and cirrhotic rat liver[7] through mammalian target of rapamycin (mTOR) signaling, a central regulator of protein synthesis, by sensing nutrient conditions.[8] Thus, peripheral amino acid composition is closely related to signaling pathways in the liver.

In addition to metabolic aspects, recent reports have elucidated new functional roles for mTOR in the IFN signaling pathway. Targeted disruptions of tuberous sclerosis 2 and eukaryotic translation initiation factor 4E binding protein 1, which both inhibit mTOR complex 1 (mTORC1) signaling, substantially enhanced IFN-alfa–dependent antiviral responses.[9,10] Therefore, mTORC1 signaling might be involved in the antiviral response as well as in metabolic processes. However, these issues have not yet been addressed in terms of IFN treatment for CH-C. In the present study, therefore, we evaluated the clinical relevance of the nutritional state of the liver, as estimated by the plasma Fischer's ratio, on Peg-IFN and RBV combination therapy. We also evaluated antiviral signaling induced by BCAA using an in vitro HCV replication system.

Materials and Methods

Patients

A total of 168 patients with CH-C at the Graduate School of Medicine at Kanazawa University Hospital (Kanazawa, Japan) and its related hospitals in Japan (Table 1, Supplementary Table 1) were evaluated in the present study. The clinical characteristics of these patients have been described previously.[4] All patients were administered Peg-IFN-alfa 2b (Schering-Plough K.K., Tokyo, Japan) and RBV combination therapy for 48 weeks. The definition of the treatment response was as follows: sustained viral response (SVR), clearance of HCV viremia 24 weeks after the cessation of therapy; transient response (TR), no detectable HCV viremia at the cessation of therapy but relapse during the follow-up period; and no response (NR). Genetic variation of the IL-28B polymorphism at rs8099917 was evaluated in all patients using TaqMan Pre-Designed SNP Genotyping Assays (Applied Biosystems, Carlsbad, CA) as described previously.[4] Gene expression profiling in the liver was performed in 91 patients using the Affymetrix Human 133 Plus 2.0 microarray chip (Affymetrix, Santa Clara, CA) as described previously (Supplementary Table 1).[4]

Plasma Amino Acid Analysis

Amino acid concentrations in plasma samples were measured by high-performance liquid chromatography–electrospray ionization–mass spectrometry, followed by derivatization.[11] Detailed experimental procedures are described in the Supplementary Materials and Methods section.

Culture Medium

Huh-7 and Huh-7.5 cells (kindly provided by Professor C. M. Rice, Rockefeller University, New York, NY) were maintained in Dulbecco's modified Eagle medium (DMEM; Gibco BRL, Gaithersburg, MD) containing 10% fetal bovine serum and 1% penicillin/streptomycin (normal medium). Amino acid-free medium (ZERO medium) was prepared by mixing 5.81 g nutrition-free DMEM (Nacalai Tesque, Kyoto, Japan), 1.85 g $NaHCO_3$, 1 g glucose, and 0.5 mL 1M (mol/L) sodium pyruvate in 500 mL Milli-Q water, then sterilizing with a 0.22-μm filter (Millipore, Billerica, MA). Low amino acid media ($\times$1/5, $\times$1/10, $\times$1/30, and $\times$1/100 DMEM) were prepared by diluting $\times$1 DMEM with ZERO medium. Powdered BCAA (leucine-isoleucine-valine, 2:1:1.2) (Ajinomoto Pharma, Tokyo, Japan) was freshly dissolved with distilled water at 100 mmol/L, then applied to cultured medium at 2 mmol/L, 4 mmol/L, or 8 mmol/L.

Western Blotting and Immunofluorescence Staining

A total of 1.5×10^5 Huh-7 cells were seeded in normal medium 24 hours before performing the experiments. The medium was changed to low-amino-acid medium and maintained for up to 24 hours. Western blotting was performed as previously described.[12] Cells were washed in phosphate-buffered saline (PBS) and lysed in RIPA buffer containing complete Protease Inhibitor Cocktail and PhosSTOP (Roche Applied Science, Indianapolis, IN). The membranes were blocked in Blocking One-P (Nacalai Tesque). The antibodies used for Western blotting are summarized in the Supplementary Materials and Methods section.

For immunofluorescence staining, cells were fixed with 4% paraformaldehyde in PBS, then permeabilized with 0.1% Triton-X 100 in PBS. The primary anti-forkhead box O (Foxo)3a antibody (Abcam, Cambridge, MA) was used at a final concentration of 2 μg/mL in PBS containing 2% fetal bovine serum at 4°C for 16 hours. Incubation with the Alexa Fluor 488–conjugated secondary antibody (Invitrogen, Carlsbad, CA) at a 500-fold dilution in PBS containing 3% fetal bovine serum antibody was performed for 4 hours, and cells were stained with Hoechst 33258 to visualize nuclear DNA (Vector Laboratories, Burlingame, CA).

Quantitative Real-Time Detection Polymerase Chain Reaction

A total of 1.5×10^5 Huh-7 cells were seeded in normal medium 24 hours before performing the experiments. The medium was changed to low-amino-acid medium, to which IFN-alfa and/or BCAA was added, and maintained for 24 hours. Rapamycin treatment (100 nmol/L) was performed for 30 minutes in normal medium before a medium change. RNA was isolated using TriPure isolation reagent (Roche Applied Science), and complementary DNA (cDNA) was synthesized using the High Capacity cDNA reverse transcription kit (Applied Biosystems, Carlsbad, CA). Real-time detection polymerase chain reaction (PCR) was performed using the 7500 Real-Time PCR System (Applied Biosystems) and Power SYBR Green PCR Master Mix (Applied Biosystems) containing specific primers according to the manufacturer's

Table 1. Comparison of Clinical Factors Between Patients With and Without NR

Clinical category	SVR+TR	NR	Univariate *P* value	Multivariate odds (95% CI)	Multivariate *P* value
Patients, n	125	43		—	
Age and sex					
Age, y	57 (30–72)	56 (30–73)	.927	—	
Sex, male vs female	68 vs 57	24 vs 19	.872	—	
Liver histology					
F stage (F1–2 vs F3–4)	95 vs 30	20 vs 23	.001	6.35 (2.02–23.7)	.001
A grade (A0–1 vs A2–3)	68 vs 57	19 vs 24	.248	—	
Host gene factors					
IL-28B (TT vs TG/GG)[a]	109 vs 12	12 vs 31	<.001	19.7 (5.74–82.7)	<.001
ISGs (Mx, IFI44, IFIT1), (<3.5 vs ≥3.5)	103 vs 22	12 vs 31	<.001	5.26 (1.65–17.6)	.005
Metabolic factors					
BMI, kg/m^2	23.2 (16.3–34.7)	23.4 (19.5–40.6)	.439	—	
TG, mg/dL	98 (30–323)	116 (45–276)	.058	—	
T-Chol, mg/dL	167 (90–237)	160 (81–214)	.680	—	
LDL-Chol, mg/dL	82 (36–134)	73 (29–123)	.019	—	
HDL-Chol, mg/dL	42 (20–71)	47 (18–82)	.098	—	
FBS, mg/dL	94 (60–291)	96 (67–196)	.139	—	
Insulin, μU/mL	6.6 (0.7–23.7)	6.8 (2–23.7)	.039	—	
HOMA-IR	1.2 (0.3–11.7)	1.2 (0.4–7.2)	.697	—	
Fischer ratio	2.3 (1.5–3.3)	2.1 (1.5–2.8)	.005	8.91 (1.62–55.6)	.011
Other laboratory parameters					
AST level, IU/L	46 (18–258)	64 (21–283)	.017	—	
ALT level, IU/L	60 (16–376)	82 (18–345)	.052	—	
γ-GTP level, IU/L	36 (4–367)	75 (26–392)	<.001	—	
WBC, /mm^3	4800 (2100–11100)	4800 (2500–8200)	.551	—	
Hb level, g/dL	14 (9.3–16.6)	14.4 (11.2–17.2)	.099	—	
PLT, ×104/mm^3	15.7 (7–39.4)	15.2 (7.6–27.8)	.378	—	
Viral factors					
ISDR mutations ≤1 vs ≥2	80 vs 44	34 vs 9	.070	4.12 (1.25–15.9)	.019
HCV-RNA, KIU/mL	2300 (126–5000)	1930 (140–5000)	.725	—	
Treatment factors					
Total dose administered					
Peg-IFN, μg	3840 (960–7200)	3840 (1920–2880)	.916	—	
RBV, g	202 (134–336)	202 (36–336)	.531	—	
Achieved administration rate					
Peg-IFN, %					
≥80%	84	28	.975	—	
<80%	42	14			
RBV (%)					
≥80%	76	24	.745	—	
<80%	50	18			
Achievement of EVR	101/125 (81%)	0/43 (0%)	<.001	—	

BMI, body mass index; CI, confidence interval; FBS, fasting blood sugar; γ-GTP, gamma-glutamyl transpeptidase; Hb, hemoglobin; HDL-chol, high density lipoprotein cholesterol; LDL-chol, low density lipoprotein cholesterol; PLT, platelets; T-chol, total cholesterol; TG, triglycerides; WBC, leukocytes.
[a]IL-28B SNP at rs8099917.

instructions. The primer sequence for real-time detection PCR is given in the Supplementary Materials and Methods section. HCV RNA was detected as described previously[12] and expression was standardized to that of glyceraldehyde-3-phosphate dehydrogenase.

Reporter Assay

Construction of the interferon stimulated response element (ISRE)-luc reporter plasmid and Socs3-luc or Socs3 (FoxO binding element mutant [FBEmut])-luc reporter plasmids is described in the Supplementary Materials and Methods section.

Huh-7 cells were transfected with the ISRE-luc reporter plasmid 24 hours before IFN-alfa treatment. Cells were treated with IFN-alfa (0 or 100 U/mL) and BCAA (2 mmol/L) in low-amino-acid media. After 24 hours, luciferase activities were measured using the Dual Luciferase assay system (Promega, Madison, WI). For Socs3 promoter activities, Huh-7 cells were transfected with Socs3-luc or Socs3 (FBEmut)-luc reporter plasmids together with the Foxo3a expression plasmid, and luciferase activities were measured after 24 hours. Values were normalized to the luciferase activity of the co-transfected pGL4.75 Renilla luciferase-expressing plasmid (Promega).

Knockdown Experiments

Huh-7 cells were transfected with Ctrl (Stealth RNAi Negative Control Low GC Duplex #2; Invitrogen) or

targets (regulatory associated protein of mTOR [Raptor] and Foxo3a) (Supplementary Materials and Methods) small interfering RNA (siRNA) using Lipofectamine RNAiMAX reagent (Invitrogen) according to the manufacturer's instructions. After 48 hours, cells were cultured in normal or low-amino-acid media for a further 24 hours. The knockdown effect was confirmed by Western blotting.

Chromatin Immunoprecipitation Assay

Detailed experimental procedures are described in the Supplementary Materials and Methods section.

HCV Replication Analysis

pH77S3 is an improved version of pH77S, a plasmid containing the full-length sequence of the genotype 1a H77 strain of HCV with 5 cell culture-adaptive mutations that promote its replication in Huh-7 hepatoma cells.[13] pH77S.3/Gaussia luciferase (GLuc)2A is a related construct in which the GLuc sequence, fused to the 2A autocatalytic protease of foot-and-mouth virus RNA, was inserted in-frame between p7 and NS2[14] (Supplementary Materials and Methods). A signal sequence in GLuc directs its secretion into cell culture media, allowing real-time, dynamic measurements of GLuc expression to be performed without the need for cell lysis.

A 10-μg aliquot of synthetic RNA transcribed from pH77S.3/GLuc2A was used for electroporation. Cells were pulsed at 260 V and 950 μF using the Gene Pulser II apparatus (Bio-Rad Laboratories, Hercules, CA) and plated in fresh normal medium for 12 hours to recover. Cell medium was changed to ×1 DMEM without serum for 8 hours, then changed to low-amino-acid medium containing 0–8 mmol/L BCAA for a further 24 hours. Cells and culture medium were collected and used for GLuc assays, real-time detection PCR, and Western blotting. The number of viable cells was determined by a (3-[4,5-dimethylthiazol-2-yl]-5-[3-carboxymethoxyphenyl]-2-[4-sulfophenyl] -2H-tetrazolium, inner salt) assay (Promega).

Continuously JFH-1–infecting Huh-7 cells were obtained by the infection of Huh-7 cells with JFH-1 cell culture-derived HCV at a multiplicity of infection of 0.01. Cells were maintained in normal medium by passaging every 3–4 days for approximately 6 months. About 20%–30% of the cells consistently were positive for HCV core protein (Supplementary Figure 4). Culture medium of JFH-1–infecting Huh-7 cells was changed to the low-amino-acid medium containing 0–8 mmol/L BCAA for 24 hours. Cells then were collected and used for assays.

Statistical Analysis

Results are expressed as mean ± standard deviation. Significance was tested by 1-way analysis of variance with the Bonferroni method, and differences were considered statistically significant at a P value of less than .05.

Results

Fischer's Ratio as a Predictive Factor for Treatment Response

The clinical characteristics of patients who received Peg-IFN and RBV combination therapy are shown in Table 1 and Supplementary Table 1, and explanations of these characteristics have been described previously.[4] All patients were infected with HCV genotype 1b and had a high viral load (>100 IU/mL). We compared patients with SVR + TR against those with NR, as assessed by the overall plausibility of treatment response groups using Fisher's C statistic as previously described.[4] We included data on the IL-28B polymorphism and plasma amino acid composition (aminogram).

Univariate regression analysis showed that no single amino acid was associated significantly with treatment response; however, using Fischer's ratio, the BCAA (Ile+Leu+Val)/aromatic amino acids (Phe+Tyr) ratio was associated significantly with treatment response (P = .005) (Table 1). Of the 121 patients with IL-28B major type, SVR, TR, and NR were observed in 53%, 37%, and 10%, respectively, and among 33 patients with IL-28B minor type, SVR, TR, and NR were observed in 15%, 17%, and 68%, respectively (P < .001) (data not shown). Fischer's ratio of SVR, TR, and NR was 2.35 ± 0.38, 2.30 ± 0.29, and 2.10 ± 0.31, respectively (P < .015) (data not shown).

We selected IL-28B polymorphism, hepatic ISG expression, fibrosis stage, HCV RNA, interferon sensitivity determining region mutation, and Fischer's ratio as factors for multivariate analysis. Multivariate analysis revealed that the minor type of IL-28B polymorphism (TG or GG at rs8099917) (odds ratio, 19.7; P < .001), advanced fibrosis stage of the liver (F3–4) (odds ratio, 6.35; P = .001), high hepatic ISGs (≧3.5) (odds ratio, 5.26; P = .005), low Fischer's ratio (continuous range, 1.5–3.3) (unit odds, 8.91; P = .011), and presence of ISDR mutation (≦1) (odds ratio, 4.12; P = .019) independently contributed to NR (Table 1).

The distribution of the Fischer's ratio according to fibrosis stage is shown in Supplementary Figure 1. The ratio decreased significantly in advanced fibrosis stage (F3–4) compared with early fibrosis stage (F1). No significant association between major or minor type of IL-28B polymorphism and different fibrosis stages of the liver was observed (Supplementary Figure 1*A*). In early fibrosis (F1–2) (Supplementary Figure 1*B*), 90% (80 of 89) of SVR+TR cases had the major type of IL-28B polymorphism, and 94% (16 of 17) of NR cases had the minor type. However, in the advanced fibrosis stage of the liver (F3–4) (Supplementary Figure 1*C*), 85% (23 of 27) of SVR+TR cases had the major type of IL-28B polymorphism and 50% (10 of 20) of NR cases had the minor type. Thus, in advanced fibrosis stages, factors other than the IL-28B polymorphism appear to contribute to NR. Interestingly, the Fischer's ratio was significantly lower in NR patients than SVR+TR pa-

tients in the advanced fibrosis stage of the liver. Therefore, Fischer's ratio could be an important predictor for NR that is independent of IL-28B polymorphism and histologic stage of the liver.

Fischer's Ratio and mTORC1 Signaling in CH-C Livers

Hepatic gene expression in 91 of 168 patients (Supplementary Table 1) was obtained using Affymetrix genechip analysis as described previously.[4] To examine the relationship between the plasma Fischer's ratio and mTORC1 signaling in the liver we evaluated the expression of key regulatory genes related to mTORC1 signaling. We found that expression of branched chain amino-acid transaminase 1 (BCAT1), an important catalytic enzyme of BCAA, was significantly negatively correlated with Fischer's ratio (Figure 1*A*). This indicates that the plasma Fischer's ratio is regulated in the liver as well as in peripheral muscle. Interestingly, the expression of c-myc, a positive regulator of BCAT1 (Figure 1*C*),[15] was correlated negatively with the Fischer's ratio (Figure 1*B*). The expression of PDCD4, a negative transcriptional target of ribosomal p70 S6 protein kinase (S6K), downstream of mTORC1, was correlated significantly with BCAT1 (Figure 1*D* and *E*). Thus, in CH-C livers, BCAT1 is induced with progressive liver disease and mTORC1 signaling is repressed, a process that might involve c-myc. Fischer's ratio of the plasma therefore can be seen to reflect mTORC1 signaling in the liver.

Impaired IFN Signaling in Huh-7 Cells Grown in Low-Amino-Acid Medium

Recent reports have shown the functional relevance of mTOR on IFN signaling and antiviral responses.[9,10] To evaluate IFN-alfa signaling and the mTOR pathway, we used Huh-7 cells grown in different amino acid conditions (×1 DMEM, ×1/5 DMEM, ×1/30 DMEM, and ×1/100 DMEM). The phosphorylated forms of mTOR (p-mTOR) and S6K (pS6K), an important downstream regulator of mTORC1 signaling, were decreased substantially in ×1/30 DMEM and ×1/100 DMEM (Figure 2*A*). Interestingly, the expression of the phosphorylated form of signal transducer and activator of transcription 1 (pSTAT1), an essential transducer of type 1 IFN signaling, also was decreased in these conditions (Figure 2*A*). Similarly, the expression of p-mTOR and pSTAT1 was repressed significantly in CH-C livers with a low Fischer's ratio compared with those with a high Fischer's ratio (Supplementary Figure 2, Supplementary Table 2).

To examine whether decreased pSTAT1 expression might be owing to repressed mTORC1 signaling, we knocked down the expression of Raptor, a specific subunit of mTORC1. We achieved more than 50% knockdown of Raptor by specific siRNA (Figure 2*B*). Under these conditions, the expression of p-mTOR and pSK6 were repressed, which is consistent with previous reports.[16] The expression of pSTAT1 also was repressed after Raptor knockdown (Figure 2*B*).

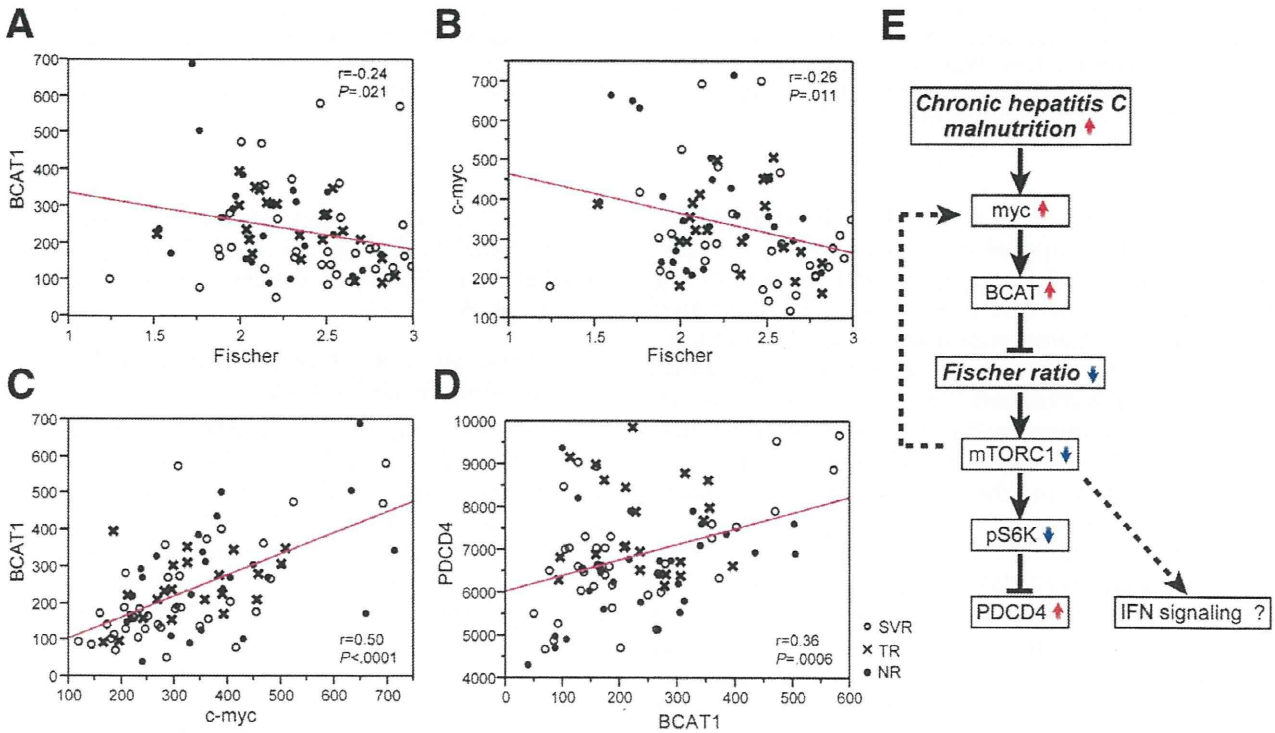

Figure 1. Regression analysis of mTORC1-related gene expression in liver. Gene expression values were determined by probe intensities. (*A*) BCAT1 and Fischer's ratio. (*B*) c-myc and Fischer's ratio. (*C*) BCAT1 and c-myc. (*D*) PDCD4 and BCAT1. (*E*) Putative signaling of mTORC1-related genes in CH-C.

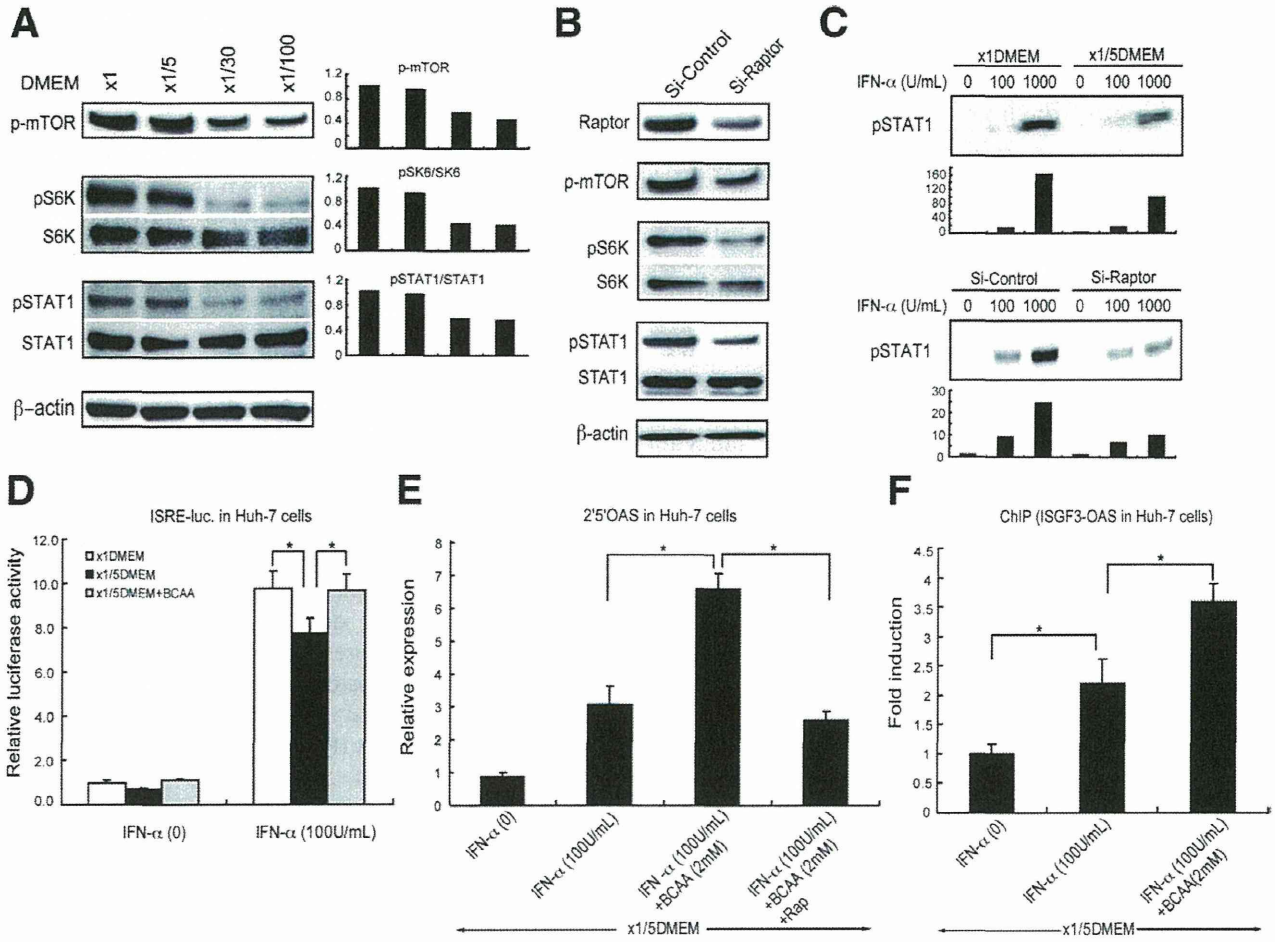

Figure 2. mTORC1 and IFN signaling in Huh-7 cells in low-amino-acid medium. (*A*) p-mTOR, pS6K, and pSTAT1 expression in different amino acid media. (*B*) p-mTOR, pS6K, and pSTAT1 expression under Raptor knock-down conditions. (*C*) IFN-alfa stimulation and pSTAT1 expression in low-amino-acid media or under Raptor knock-down conditions. (*D*) IFN-alfa stimulation and ISRE reporter activities in normal and low amino-acid media. (*E*) IFN-alfa stimulation and 2'5'OAS expression supplemented with BCAA or rapamycin in low-amino-acid medium. (*F*) Chromatin immunoprecipitation of 2'5'OAS promoter region by ISGF3γ.

The induction of pSTAT1 by IFN-alfa (1000 U/mL) stimulation was impaired in ×1/5 DMEM or in Raptor knocked-down condition, compared with the control (Figure 2*C*). Consistent with these results, IFN-alfa–induced ISRE-dependent transcriptional activity, as measured using an ISRE-luciferase reporter assay, was impaired significantly in ×1/5 DMEM compared with ×1 DMEM (Figure 2*D*). However, this activity could be rescued by the addition of 2 mmol/L BCAA (Figure 2*D*). These results were confirmed by determining the expression of the endogenous IFN-alfa responsive gene, 2'5'OAS, using quantitative reverse-transcription PCR. Figure 2*E* shows that BCAA treatment augmented 2'5'OAS expression in low levels of amino acids, and that this could be reversed by the addition of rapamycin, an inhibitor of mTORC1 (Figure 2*E*). Furthermore, chromatin immunoprecipitation (ChIP) experiments revealed that transcriptional augmentation by BCAA was mediated by the binding of the IFN-alfa–inducible transcription factor, ISGF3γ, to the promoter region of 2'5'OAS (Figure 2*F*). These results indicate that amino acids in culture media play an essential role in IFN-alfa signaling through mTORC1 signaling, and that the addition of BCAA can overcome impaired IFN-alfa signaling in Huh-7 cells.

Induction of Socs3 in Low-Amino-Acid Medium in Huh-7 Cells

Besides being involved in mTOR signaling, Foxo transcriptional factors mediate another important branch of nutrition-sensing signaling pathway.[17] Therefore, we evaluated forkhead box O3A (Foxo3a) expression in low-amino-acid conditions in Huh-7 cells. After 6 hours culture in ×1/5, ×1/30, and ×1/100 DMEM, expression of the phosphorylated form of Foxo3a (pFoxo3a) decreased, whereas that of total Foxo3a increased in ×1/5 and ×1/30 DMEM, and the ratio of pFoxo3a to Foxo3a (pFoxo3a/Foxo3a) substantially decreased (Figure 3*A* and *B*). It has been reported that dephosphorylated Foxo3a is translocated to the nucleus before activation of its target genes.[18] In the present study, immunofluorescent staining

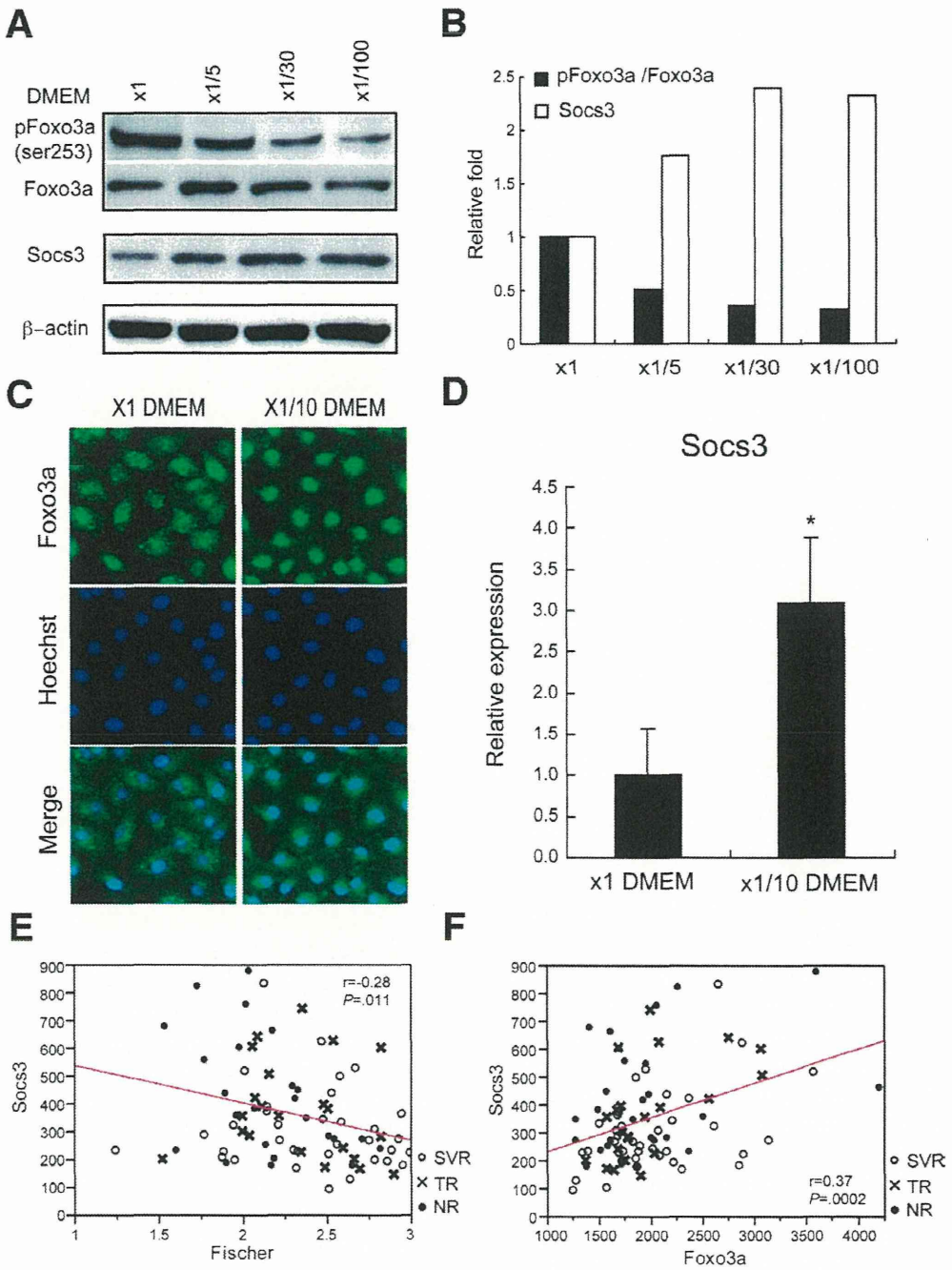

Figure 3. Foxo3a and Socs3 signaling in Huh-7 cells in low-amino-acid medium. (*A*) Foxo3a and Socs3 expression in different amino acid media. (*B*) Relative change of pFoxo3a/Foxo3a and Socs3 expression in different amino acid media. (*C*) Immunofluorescence staining of Foxo3a in Huh-7 cells in normal and low-amino-acid media. (*D*) Relative change of Socs3 messenger RNA in Huh-7 cells in normal and low-amino-acid media. (*E*) Regression analysis of Socs3 in liver and Fischer's ratio. (*F*) Regression analysis of Socs3 and Foxo3a in liver.

with an anti-Foxo3a antibody showed that Foxo3a diffused in both the cytoplasm and nucleus in normal amino acid medium, but localized in the nucleus in low-amino-acid medium (×1/10 DMEM) (Figure 3*C*).

Interestingly, in low-amino-acid medium, transcription and protein expression of Socs3 increased significantly (Figure 3*A*, *B*, and *D*). The induction of Socs3 in a state of malnutrition also was confirmed in clinical samples. In CH-C livers there was a significant negative correlation between the plasma Fischer's ratio and Socs3 expression, implying that Socs3 expression increases during the malnutrition state induced by CH-C. There was also a significant correlation between Foxo3a and the transcriptional level of Socs3 in CH-C livers (Figure 3*E* and *F*), suggesting an in vitro and in vivo biological role for Foxo3a in the activation of Socs3 expression. These findings also were confirmed by Western blotting of CH-C livers (Supplementary Figure 2, Supplementary Table 2).

Socs3 Is a Transcriptional Target of Foxo3a

The significant correlation between Socs3 and Foxo3a in CH-C livers prompted us to analyze the Socs3 promoter sequence and, in doing so, we identified a putative Foxo binding element (FBE) (Figure 4*A*). To investigate the functional relevance of Foxo3a in the transcriptional regulation of Socs3, we constructed reporter plasmids containing a luciferase coding region fused to the Socs3 promoter region (Socs3-luc). Socs3-luc promoter activity was increased substantially by the overexpression of Foxo3a (Figure 4*B*). The mutations introduced in the putative FBE (FBEmut) in the Socs3 promoter significantly reduced Foxo3a-induced Socs3 promoter activation (Figure 4*B*).

Foxo3a then was knocked down by siRNA and Socs3 induction was evaluated. After suppression of Foxo3a (Supplementary Figure 3), Socs3 promoter activity was repressed significantly in low-amino-acid medium (×1/10 DMEM) (Figure 4*C*). Thus, Foxo3a appears to be indispensable for activating the Socs3 promoter under low-amino-acid conditions. Correlating with these results, ChIP assays using an anti-Foxo3a antibody showed a significant increase in the association between Foxo3a and the FBE of the Socs3 promoter in low-amino-acid conditions (×1/10 DMEM) (Figure 4*D*). Taken together, these results suggest that, besides mTORC1 signaling, the Foxo3a-mediated Socs3 signaling pathway might contribute to impaired IFN signaling in a state of malnutrition in CH-C. BCAA potentially restores this signaling (Figure 4*E*).

Effect of BCAA on HCV Replication in Huh-7 or Huh-7.5 Cells

Based on the earlier-described results, we used 2 HCV in vitro replication systems to examine whether BCAA affects HCV replication in Huh-7 or Huh-7.5 cells. The first system used a recombinant infectious genotype 1a clone, H77S.3/GLuc2A (Supplementary Materials and Methods, Supplementary Figure 4), including reporter genes, whereas the second used continuously JFH-1–infecting Huh-7 cells (Supplementary Materials and Methods).

The synthetic RNA transcribed from pH77S.3/GLuc2A was introduced into Huh-7.5 cells and replication of H77S.3/GLuc2A was evaluated in normal or low-amino-acid medium supplemented with BCAA. H77S.3/GLuc2A increased significantly by 2.6-fold in Huh-7.5 cells grown in low-amino-acid medium (×1/5 DMEM) compared with normal amino acid medium (×1 DMEM). Interestingly, BCAA repressed H77S.3/GLuc2A replication in a dose-dependent manner (Figure 5*A*). In agreement with these results, the expression of Mx-1 was increased significantly by the addition of BCAA (Figure 5*B*). Similar findings were observed in JFH-1–infecting Huh-7 cells (Materials and Methods, Supplementary Figure 4). Although no obvious increase in HCV replication was observed in low-amino-acid medium (×1/5 DMEM) compared with normal amino acid medium (×1 DMEM), JFH-1 replication was repressed significantly by the addition of BCAA in a dose-dependent manner (Figure 5*D*). The expression of Mx-1 was increased substantially by the addition of BCAA (Figure 5*E*), suggesting that BCAA significantly repressed HCV replication in cells with either naive or persistent HCV infection. Importantly, there were no significant differences in cell viability between the conditions (Figure 5*C* and *F*).

To validate these findings, signaling pathways in HCV replicating cells were examined (Figure 6*A* and *B*). BCAA increased pS6K in a dose-dependent manner, implying its involvement in the activation of mTORC1 signaling. Related to this, expression of pSTAT1 was shown to be increased and the ratio of pSTAT1 to total STAT1 (pSTAT1/STAT1) increased 2.5- to 3-fold after the addition of BCAA. Thus, BCAA activated mTORC1 and the JAK-STAT signaling pathway in HCV-infected cells. In addition, the expression ratio of pFoxo3a to total Foxo3a (pFoxo3a/Foxo3a) increased 3- to 4-fold, indicating an increase in the cytoplasmic form of Foxo3a that is exposed to proteasome degradation. Concordant with these findings, we observed a decrease in the expression of Socs3. In addition, expression of the HCV core protein decreased as shown in Figure 6*A* and *B*. Thus, these results clearly show that BCAA repressed HCV replication through activation of IFN signaling and repression of Socs3-mediated IFN inhibitory signaling, as proposed in Figure 4*E*.

Discussion

Thompson et al[5] showed that the IL-28B polymorphism, HCV RNA, nationality (Caucasian/Hispanic vs African American), hepatic fibrosis stage, and fasting blood sugar level are all significant variables for achieving SVR in patients infected with genotype 1 HCV. However, the significance of variable factors for treatment response in conjunction with the IL-28B polymorphism has not been evaluated fully. In the present study, in addition to previously examined variables,[4] we included the plasma Fischer's ratio as a nutritional parameter. Multivariate analysis showed that the minor type of IL-28B polymorphism, advanced fibrosis stage, high hepatic ISGs, low Fischer's ratio, and ISDR mutation (≤1) independently contributed to NR (Table 1). Interestingly, among patients of similar fibrosis stage (F3–4), the Fischer's ratio was significantly lower in NR than SVR+TR cases. Therefore, the plasma value of Fischer's ratio was associated with the treatment response that was independent of the IL-28B polymorphism and histologic stage of the liver, although patients with advanced hepatic fibrosis are likely to be nutritionally affected.

As a nutrient sensor signaling pathway, the protein kinase mTOR plays an essential role in maintaining homeostasis and regulates protein synthesis in response to nutrient conditions. mTOR is the catalytic subunit of 2 distinct complexes, mTORC1 and mTORC2. In addition

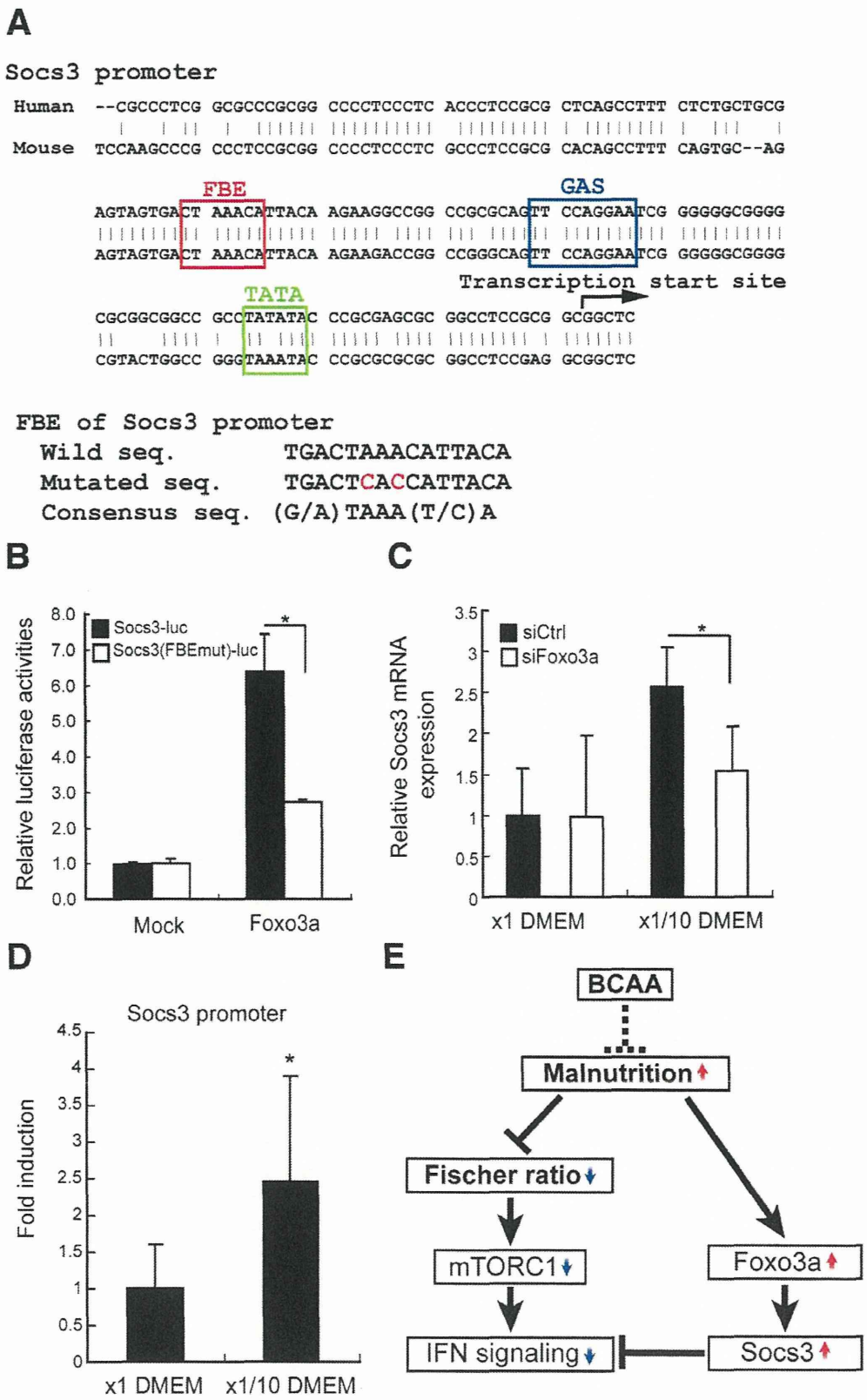

Figure 4. Socs3 promoter assay. (*A*) Primary structure of putative Foxo binding element in Socs3 promoter region. (*B*) Socs3-luc and Socs3 (FBEmut)-luc activities after overexpression of Foxo3a in Huh-7 cells. (*C*) Relative Socs3 messenger RNA (mRNA) expression after knockdown of Foxo3a in normal and low-amino-acid media. (*D*) Chromatin immunoprecipitation of Socs3 promoter region by Foxo3a in normal and low-amino-acid media. (*E*) Model of impaired IFN signaling by repressed mTORC1 signaling and increased Socs3 signaling under CH-C state of malnutrition.

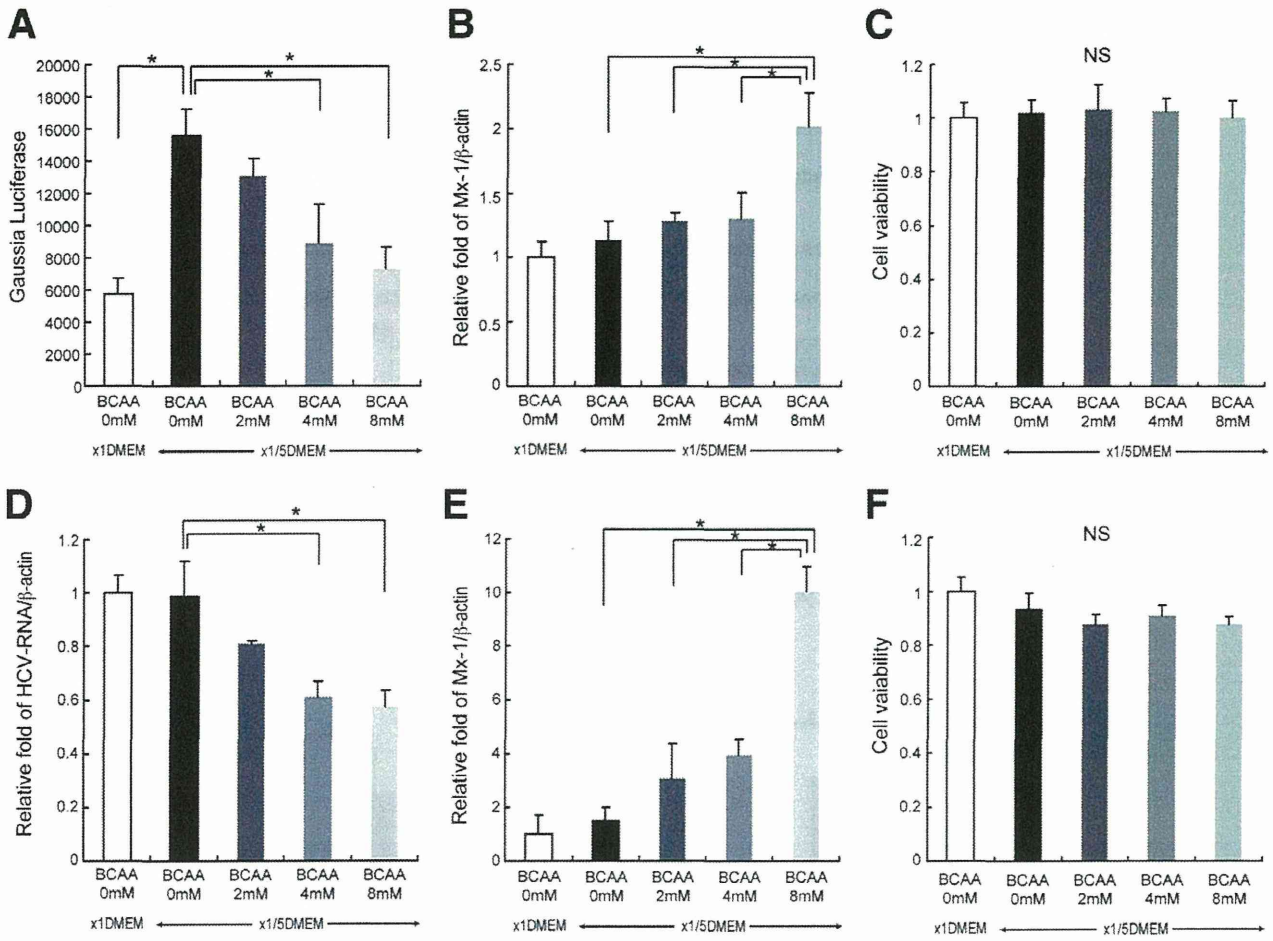

Figure 5. Effect of BCAA on HCV replication in cells in low-amino-acid medium. (*A*) Effect of BCAA on H77S.3/GLuc2A replication in Huh-7.5 cells. (*B*) Mx-1 expression in H77S.3/GLuc2A-transfected Huh-7.5 cells supplemented with BCAA. (*C*) Viability of Huh-7.5 cells. (*D*) Effect of BCAA on JFH-1 replication continuously infecting Huh-7 cells. (*E*) Mx-1 expression in continuously JFH-1–infecting Huh-7 cells supplemented with BCAA. (*F*) Viability of Huh-7 cells.

to these metabolic aspects, recent reports have shown that mTORC1 participates in IFN signaling and antiviral defense responses,[9,10] although the precise signaling pathway has not yet been clarified. In the present study, we evaluated mTORC1 signaling in CH-C livers using gene expression profiling of 91 patients (Figure 1, Supplementary Table 1). We observed a significant negative correlation between plasma Fischer's ratio and hepatic expression of BCAT1, an important catalytic enzyme of BCAA (Figure 1*A*). Moreover, BCAT1 expression was correlated positively with PDCD4 expression, which in turn is regulated negatively by pS6K at the transcriptional level (Figure 1*D*).[16] Thus, the expression of BCAT1 appears to be a negative indicator of mTORC1 signaling in the liver, and the plasma Fischer's ratio is partially reflected by mTORC1 signaling in the liver and muscle.

Interestingly, the expression of c-myc was correlated significantly with BCAT1 (Figure 1*C*) as reported previously.[15] Several studies observed up-regulated c-myc expression in advanced stages of CH-C[19] but, on the other hand, c-myc recently was shown to be a target of mTORC1 in hepatic cells.[17] The existence of a feedback mechanism between c-myc and mTORC1 signaling to maintain liver homeostasis (Figure 1*E*) is plausible, although the precise mechanisms need to be confirmed.

Impaired mTORC1 signaling is suggested to affect the IFN-alfa–induced signaling pathway. To address this, the relationship between mTORC1 and IFN signaling was assessed using a cell culture system. In low-amino-acid medium (×1/5, ×1/30, and ×1/100 DMEM), expression of pSTAT1 was decreased substantially, correlating with the impaired mTORC1 signaling represented by decreased p-mTOR and pS6K expression in Huh-7 cells (Figure 2*A*).

The relationship between mTORC1 and IFN signaling was confirmed further by the knock-down experiment of Raptor, a specific subunit of mTORC1 (Figure 2*B*), although a more precise analysis should be performed to confirm this relationship. Importantly, when Huh-7 cells were stimulated by IFN-alfa, pSTAT1 induction was repressed significantly in low-amino-acid medium (×1/5 DMEM) or in Raptor knocked-down conditions (Figure 2*C*). It therefore could be speculated that IFN treat-

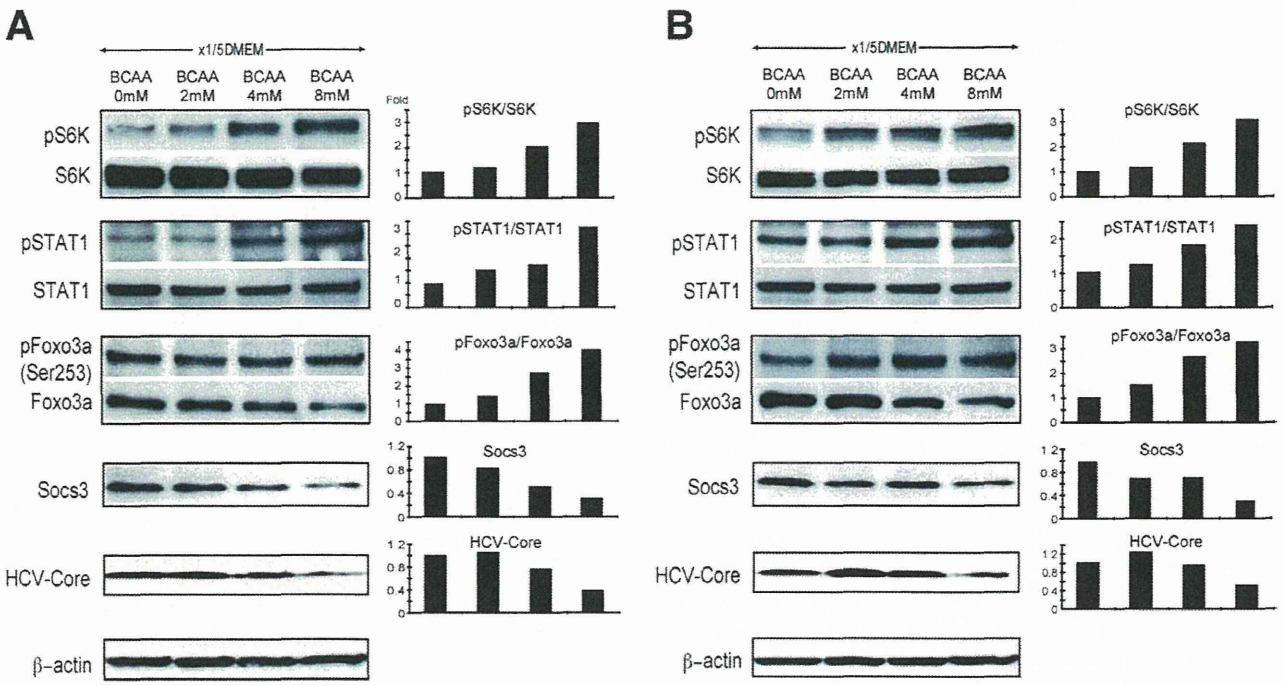

Figure 6. Expression of S6K, STAT1, Foxo3a, Socs3, and HCV core in H77S.3/GLuc2A-transfected Huh-7.5 cells or continuously JFH-1–infecting Huh-7 cells supplemented with BCAA.

ment of patients with liver malnutrition and impaired mTORC1 signaling would lead to reduced induction of ISGs. Importantly, BCAA was able to restore impaired IFN signaling through increased binding of ISGF3γ to its targets (Figure 2*D–F*).

Besides cross-talk of mTORC1 and IFN signaling, we revealed that Foxo3a also is involved in the IFN inhibitory pathway. In low-amino-acid medium, expression of pFoxo3a (ser253) was decreased substantially whereas that of Socs3 was increased. A decreased pFoxo3a/Foxo3a ratio indicates nuclear accumulation of Foxo3a before activation of its target genes, and this was confirmed by immunofluorescent staining (Figure 3*C*). The expression of Foxo3a was significantly positively correlated with that of Socs3 in CH-C liver (Figure 3*F*). These findings prompted us to identify a putative FBE in the Socs3 promoter region (Figure 4*A*). In fact, Socs3 promoter reporter activity was activated by overexpression of Foxo3a, and mutation of FBE impaired Foxo3a-dependent Socs3 promoter activation. Conversely, induction of Socs3 was not observed when expression of Foxo3a was knocked down by siRNA in low-amino-acid medium. Socs3 induction in low-amino-acid medium was owing to increased binding of Foxo3a to the FBE, which was confirmed by ChIP (Figure 4*D*). Therefore, in addition to impaired mTORC1 signaling, the Foxo3a-mediated Socs3 IFN inhibitory pathway might be involved in impaired IFN signaling in patients with liver malnutrition (Figure 4*E*).

Finally, we examined whether BCAA could restore impaired IFN signaling and inhibit HCV replication in cells under conditions of malnutrition. Importantly, BCAA could repress replication of the recombinant genotype 1a-derived HCV, H77S.3/GLuc2A, in a dose-dependent manner (Figure 5*A*). H77S.3/GLuc2A RNA produces infectious virus[14] and, therefore, the results indicate that BCAA might act on a naive HCV infection. Moreover, BCAA inhibited JFH-1–infected Huh-7 cells in which JFH-1 continuously was infecting in a dose-dependent manner. These results indicate that BCAA had an inhibitory effect on either naive or persistent HCV infection irrespective of genotypes (1a and 2a). Consistent with these results, BCAA induced the expression of pSTAT1 and Mx protein in a dose-dependent manner, and repressed Socs3 expression through increasing the ratio of pFoxo3a (ser243) to Foxo3a in a dose-dependent manner (Figures 5 and 6). Therefore, BCAA potentially could restore impaired IFN signaling and inhibit HCV replication in a CH-C state of malnutrition.

In conclusion, we addressed the clinical significance of the nutritional state of the liver on the treatment response of Peg-IFN and RBV combination therapy for CH-C. Although further studies are required to fully define the precise mechanisms underlying mTOR and IFN signaling, we showed that plasma values of Fischer's ratio are a useful nutritional parameter associated with treatment response. Fischer's ratio reflects mTORC1 signaling in the liver, which is correlated with IFN signaling and related to Socs3 IFN inhibitory signaling through Foxo3a. The potential usefulness of BCAA for the augmentation of IFN signaling could suggest a new therapeutic application for advanced-stage CH-C.

Supplementary Material

Note: To access the supplementary material accompanying this article, visit the online version of *Gastroenterology* at www.gastrojournal.org, and at doi: 10.1053/j.gastro.2011.03.051.

Appendix A

The Hokuriku Liver Study Group is composed of the following members: Drs Takashi Kagaya, Kuniaki Arai, Kaheita Kakinoki, Kazunori Kawaguchi, Hajime Takatori, and Hajime Sunakosaka (Department of Gastroenterology, Kanazawa University Graduate School of Medicine, Kanazawa, Japan); Drs Touru Nakahama and Shinji Kamiyamamoto (Kurobe City Hospital, Kurobe, Toyama, Japan); Dr Yasuhiro Takemori (Toyama Rosai Hospital, Uozu, Toyama, Japan); Dr Hikaru Oguri (Koseiren Namerikawa Hospital, Namerikawa, Toyama, Japan); Drs Yatsugi Noda and Hidero Ogino (Toyama Prefectural Central Hospital, Toyama, Japan); Drs Yoshinobu Hinoue and Keiji Minouchi (Toyama City Hospital, Toyama, Japan); Dr Nobuyuki Hirai (Koseiren Takaoka Hospital, Takaoka, Toyama, Japan); Drs Tatsuho Sugimoto and Koji Adachi (Tonami General Hospital, Tonam, Toyama, Japan); Dr Yuichi Nakamura (Noto General Hospital, Nanao, Ishikawa, Japan); Drs Masashi Unoura and Ryuhei Nishino (Public Hakui Hospital, Hakui, Ishikawa, Japan); Drs Hideo Morimoto and Hajime Ohta (National Hospital Organization Kanazawa Medical Center, Kanazawa, Ishikawa, Japan); Dr Hirokazu Tsuji (Kanazawa Municipal Hospital, Kanazawa, Ishikawa, Japan); Drs Akira Iwata and Shuichi Terasaki (Kanazawa Red Cross Hospital, Kanazawa, Ishikawa, Japan); Drs Tokio Wakabayashi and Yukihiro Shirota (Saiseikai Kanazawa Hospital, Kanazawa, Ishikawa, Japan); Drs Takeshi Urabe and Hiroshi Kawai (Public Central Hospital of Matto Ishikawa, Hakusan, Ishikawa, Japan); Dr Yasutsugu Mizuno (Nomi Municipal Hospital, Nomi, Ishikawa, Japan); Dr Shoni Kameda (Komatsu Municipal Hospital, Komatsu Ishikawa, Japan); Drs Hirotoshi Miyamori and Uichiro Fuchizaki (Keiju Medical Center, Nanao, Ishikawa, Japan); Dr Haruhiko Shyugo (Kanazawa Arimatsu Hospital, Kanazawa, Ishikawa, Japan); Dr Hideki Osaka (Yawata Medical Center, Komatsu, Ishikawa, Japan); Dr Eiki Matsushita (Kahoku Central Hospital, Tsubata, Ishikawa, Japan); Dr Yasuhiro Katou (Katou Hospital, Komatsu, Ishikawa, Japan); Drs Nobuyoshi Tanaka and Kazuo Notsumata (Fukuiken Saiseikai Hospital, Fukui, Japan); Dr Mikio Kumagai (Kumagai Clinic, Tsuruga, Fukui, Japan); and Dr Manabu Yoneshima (Municipal Tsuruga Hospital, Tsuruga, Fukui, Japan).

References

1. Fried MW, Shiffman ML, Reddy KR, et al. Peginterferon alfa-2a plus ribavirin for chronic hepatitis C virus infection. N Engl J Med 2002;347:975–982.
2. Tanaka Y, Nishida N, Sugiyama M, et al. Genome-wide association of IL28B with response to pegylated interferon-alpha and ribavirin therapy for chronic hepatitis C. Nat Genet 2009;41: 1105–1109.
3. Ge D, Fellay J, Thompson AJ, et al. Genetic variation in IL28B predicts hepatitis C treatment-induced viral clearance. Nature 2009;461:399–401.
4. Honda M, Sakai A, Yamashita T, et al. Hepatic ISG expression is associated with genetic variation in interleukin 28B and the outcome of IFN therapy for chronic hepatitis C. Gastroenterology 2010;139:499–509.
5. Thompson AJ, Muir AJ, Sulkowski MS, et al. Interleukin-28B polymorphism improves viral kinetics and is the strongest pretreatment predictor of sustained virologic response in genotype 1 hepatitis C virus. Gastroenterology 2010;139:120–129 e18.
6. Nishitani S, Ijichi C, Takehana K, et al. Pharmacological activities of branched-chain amino acids: specificity of tissue and signal transduction. Biochem Biophys Res Commun 2004;313:387–389.
7. Matsumura T, Morinaga Y, Fujitani S, et al. Oral administration of branched-chain amino acids activates the mTOR signal in cirrhotic rat liver. Hepatol Res 2005;33:27–32.
8. Kim DH, Sarbassov DD, Ali SM, et al. mTOR interacts with raptor to form a nutrient-sensitive complex that signals to the cell growth machinery. Cell 2002;110:163–175.
9. Colina R, Costa-Mattioli M, Dowling RJ, et al. Translational control of the innate immune response through IRF-7. Nature 2008;452: 323–328.
10. Kaur S, Lal L, Sassano A, et al. Regulatory effects of mammalian target of rapamycin-activated pathways in type I and II interferon signaling. J Biol Chem 2007;282:1757–1768.
11. Shimbo K, Kubo S, Harada Y, et al. Automated precolumn derivatization system for analyzing physiological amino acids by liquid chromatography/mass spectrometry. Biomed Chromatogr 2009; 24:683–691.
12. Shirasaki T, Honda M, Mizuno H, et al. La protein required for internal ribosome entry site-directed translation is a potential therapeutic target for hepatitis C virus replication. J Infect Dis 2010;202:75–85.
13. Yi M, Villanueva RA, Thomas DL, et al. Production of infectious genotype 1a hepatitis C virus (Hutchinson strain) in cultured human hepatoma cells. Proc Natl Acad Sci U S A 2006;103:2310–2315.
14. Shimakami T, Welsch C, Yamane D, et al. Protease inhibitor-resistant hepatitis C virus mutants with reduced fitness from impaired production of infectious virus. Gastroenterology 2011; 140:667–675.
15. Eden A, Simchen G, Benvenisty N. Two yeast homologs of ECA39, a target for c-Myc regulation, code for cytosolic and mitochondrial branched-chain amino acid aminotransferases. J Biol Chem 1996; 271:20242–2045.
16. Dowling RJ, Topisirovic I, Alain T, et al. mTORC1-mediated cell proliferation, but not cell growth, controlled by the 4E-BPs. Science 2010;328:1172–1176.
17. Teleman AA, Hietakangas V, Sayadian AC, et al. Nutritional control of protein biosynthetic capacity by insulin via Myc in Drosophila. Cell Metab 2008;7:21–32.
18. Zhang X, Gan L, Pan H, et al. Phosphorylation of serine 256 suppresses transactivation by FKHR (FOXO1) by multiple mechanisms. Direct and indirect effects on nuclear/cytoplasmic shuttling and DNA binding. J Biol Chem 2002;277: 45276–45284.
19. Farinati F, Cardin R, Bortolami M, et al. Oxidative damage, pro-inflammatory cytokines, TGF-alpha and c-myc in chronic HCV-related hepatitis and cirrhosis. World J Gastroenterol 2006;12: 2065–2069.

Received October 19, 2010. Accepted March 18, 2011.

Reprint requests

Address requests for reprints to: Shuchi Kaneko, MD, PhD, Department of Gastroenterology, Graduate School of Medicine, Kanazawa University, Takara-Machi 13-1, Kanazawa 920-8641, Japan. e-mail: skaneko@m-kanazawa.jp; e-mail: fax: (81) 76-234-4250.

Acknowledgments

Participating investigators from the Hokuriku Liver Study Group are listed in Appendix A.

The authors thank Mina Nishiyama and Yuki Hatayama for excellent technical assistance.

Conflicts of interest

The authors disclose no conflicts.

Supplementary Materials and Methods

Plasma Amino Acid Analysis

Plasma sample amino acid concentrations were measured by high-performance liquid chromatography-electrospray ionization-mass spectrometry followed by derivatization.[1] An MSQ Plus LC/MS system (Thermo Fischer Scientific, Waltham, MA) equipped with an electrospray ionization source was used in positive ionization mode for selected ion monitoring. Xcalibur version 1.4 SR1 software (Thermo Fischer Scientific, Yokohama, Japan) was used for data collection and processing. The high-performance liquid chromatography separation system consisted of an L-2100 pump, L-2200 autosampler, and L-2300 column oven (Hitachi High-Technologies Corporation, Tokyo, Japan). A Wakosil-II 3C8-100HG column (100, 2.1, 3 mm; Wako Pure Chemical Industries, Osaka, Japan) was used for the separation, and the mobile phase consisted of eluent A (25-mmol/L ammonium formate in water, pH 6.0) and eluent B (water:acetonitrile = 40:60).

Western Blotting

The expression of HCV core protein, Socs3, Foxo3a, phospho-Foxo3a (Ser253) (pFoxo3a), STAT1, pSTAT1 (Tyr701), S6K, pS6K, p-mTOR (Ser2448), Raptor, and β-actin were evaluated with mouse anti-core (Affinity BioReagents, Golden, CO), mouse anti-Socs3 (Santa Cruz Biotechnology, Santa Cruz, CA), rabbit anti-Foxo3a, rabbit anti-β-actin (Sigma-Aldrich, St Louis, MO), rabbit anti-phospho-Foxo3a (Ser253), rabbit anti-STAT1, rabbit anti-p-STAT1 (Tyr701), rabbit anti-p70 S6K, rabbit anti-pS6K, rabbit anti-p-mTOR (Ser2448), and rabbit anti-Raptor (Cell Signaling Technology, Beverly, MA), respectively. Densitometric analysis was conducted directly on the blotted membrane using a charge coupled device camera system (LAS-3000 Mini; Fujifilm, Tokyo, Japan) and Scion Image software (Frederick, MD).

Primer Sequences for PCR and siRNA

Primer sequences for PCR and siRNA were as follows: 2′5′OAS: forward 5′- CTC AGA AAT ACC CCA GCC AAA TC-3′, reverse 5′-GTG GTG AGA GGA CTG AGG AA-3′; Socs3: forward 5′-TAC CAC CTG AGT CTC CAG CTT CTC-3′, reverse 5′-CCT GGC AGT TCT CAT TAG TTC AGC ATT C-3′; Foxo3a: forward 5′-TGC TGT ATG CAA GAA CTT TCC AGT AGC AG-3′, reverse 5′-ACT CTA GCC CCC ATG CTA CTA GTG-3′; glyceraldehyde-3-phosphate dehydrogenase: forward 5′-GAA GGT GAA GGT CGG AGT-3′, reverse 5′-GAA GAT GGT GAT GGG ATT TC-3′, siFoxo3a (SASI_Hs01_00119127; Sigma) sense: 5′-GAA UGA UGG GCU GAC UGA AdTdT-3′, antisense: 5′-UUC AGU CAG CCC AUC AUU CdTdT-3′. Small interfering Raptor was purchased as part of KIAA1303 siGENOME SMART pool siRNA reagents from Dharmacon, Inc (Lafayette, CO).

Construction of ISRE-Luc Reporter and FBEmut-luc Reporter Plasmids

Oligonucleotides containing the ISRE tandem repeat sequence (sense 5′-TCG AGA ACT GAA ACT GAA ACT GAA ACT GAA ACT GAA ACT GAA ACT GAA ACT GAA A-3′, antisense 5′-AGC TTT TCA GTT TCA GTT TCA GTT TCA GTT TCA GTT TCA GTT TCA GTT TCA GTT C-3′, consensus 5′-GAA Ann GAA ACT-3′) were annealed, and integrated into Xho I and Hind III sites of the pGL4.23 luciferase vector (Promega). The human Socs3 promoter region (-109/+217) was amplified by genomic PCR using specific primers (forward, 5′-TGC TGC GAG TAG TGA CTA AAC ATT ACA AG-3′ and reverse, 5′-CCG TGA AGT CCA CAA AGG AGC CTT C-3′) and cloned into the EcoR V site of the pGL4.10-luc2 reporter vector (Promega). The Socs3 FBE mutant reporter vector was created by substituting 2 adenines in the putative FBE with guanines (wild-type sequence 5′-CTAAACA-3′, mutated sequence 5′-CTGAGCA-3′).

ChIP Assay

For the ChIP assay using the anti-ISGF3γ antibody, 1×10^6 Huh-7 cells were treated with IFN-alfa (0 or 100 U/mL) and BCAA (2 mmol/L) in low-amino-acid medium for 6 hours. For ChIP using the anti-Foxo3a antibody, 1×10^6 Huh-7 cells were cultured in low-amino-acid medium for 24 hours.

Cells were cross-linked with 1% formaldehyde in PBS for 10 minutes at 37°C, and the reaction was stopped with 250 mmol/L glycine for 10 minutes. Cells were suspended in sodium dodecyl sulfate-lysis buffer (1% sodium dodecyl sulfate, 10 mmol/L ethylenediaminetetraacetic acid [EDTA], 50 mmol/L Tris-HCl [pH 8.1]), complete protease inhibitor cocktail (Roche Applied Science), and incubated for 30 minutes at 10°C. Cell lysate was sonicated with Bioruptor (Cosmo Bio, Tokyo, Japan) to obtain chromatin fragments and diluted 10-fold in ChIP dilution buffer (0.01% sodium dodecyl sulfate, 1.1% Triton-X 100, 1.2 mmol/L EDTA, 16.7 mmol/L Tris-HCl [pH 8.1], 150 mmol/L NaCl, complete protease inhibitor cocktail). Chromatin fragments were incubated with 2 μg ISGF3γ antibody (Santa Cruz Biotechnology), 2 μg Foxo3a antibody (H-144; Santa Cruz Biotechnology), or normal rabbit immunoglobulin G for 18 hours at 4°C. Dynabeads (30 μL) protein G (Invitrogen) was added and incubated for 1 hour at 4°C. The beads were washed with low-salt-wash buffer (0.1% sodium dodecyl sulfate, 1% Triton-X 100, 2.0 mmol/L EDTA, 20 mmol/L Tris-HCl [pH 8.1], 150 mmol/L NaCl), high-salt-wash buffer (0.1% sodium dodecyl sulfate, 1% Triton-X 100, 2.0 mmol/L EDTA, 20 mmol/L Tris-HCl [pH 8.1], 500 mmol/L NaCl), LiCl wash buffer (250 mmol/L LiCl, 1% NP-40, 1% de-